GEAR TECHNOLOGY

NOVEMBER/DECEMBER 2001

The Journal of Gear Manufacturing

www.geartechnology.com

FEATURES

- Dry Shaping
- Profile Shift
- Oil additives and EHL Film Thickness
- Gear Power Honing and Tooth Properties

CD-ROM BUYERS GUIDE ISSUE

The Gear Industry on your desktop!

THE GEAR INDUSTRY'S INFORMATION SOURCE

GEAR CUTTING & TESTING

Bevel gear cutting enters a new era with the PHOENIX® II 275HC CNC Bevel Gear Cutting Machine.

It's 35% smaller than the Phoenix® 175HC but produces parts with diameters up to 275 mm...cuts dry without chip shrouds and vacuum systems... simplifies and speeds part load/ unload and cutter changeover... and features direct-drive spindle motors for faster setup and machining times.

Thanks to a breakthrough monolithic column design, all of these user benefits are now available, and much more.

In short, the new PHOENIX® II 275HC picks up where its 175HC predecessor left off— and leaves competitive machines completely in the dust.

Machine Footprint Comparison

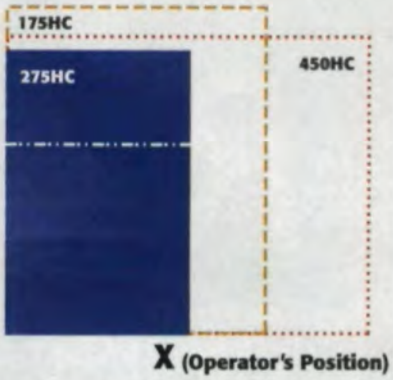

PHOENIX® II 275HC occupies just 90 sq. ft.; 35% less floorspace than the 175HC, and far less than competitive machines.

New 600HTT TURBO TESTER™ performs faster CNC-controlled roll testing of spiral and hypoid bevel gear sets.

It features a small footprint, ergonomic and easy-to-use design...performs not only basic pattern checking but also SFT (Single Flank Transmission error) testing and SBN (Structure-Borne-Noise) testing...and accommodates workpiece diameters up to 600 mm.

These and many other user benefits are now possible with the 600HTT TURBO TESTER™. It shares the same platform made popular with the recent introduction of the 600HTL TURBO LAPPER™, so you benefit from vast reductions in floorspace, and a highly accessible work chamber.

Leave it to Gleason to take bevel gear cutting and testing to the next level.

The Gleason Works

1000 University Ave., P.O. Box 22970
Rochester, NY 14692-2970 U.S.A.
Phone: 716/473-1000 Fax: 716/461-4348
Web site: www.gleason.com
E-mail: sales@gleason.com

CIRCLE 110


SHAPER CUTTER RESHARPENING IS NOW AVAILABLE AT STAR CUTTER!
NOW AVAILABLE FROM STAR CUTTER COMPANY
Star Resharpening
Star Resharpening for Hobs and Form Relieved Milling Cutters... from a Leading Manufacturer of Hobs and Form Relieved Milling Cutters and Tool Grinding Machines. And now Shaper Cutter Resharpening is available at Star Cutter...The Number One Choice for Resharpening Services.
www.starcutter.com
email: resharp@starcutter.com
Phone: 1-888-Resharp
Fax: 1-989-345-5660
ISO 9001 REGISTERED
SIGMA POOL
AGMA
Since 1927
Star®
STAR CUTTER COMPANY
West Branch Industries.
A subsidiary of Star Cutter Company.
2083 M55, West Branch Michigan, 48661
Telephone Toll Free 888-RESHARP
Fax 517-345-5660
CIRCLE 132

GEAR TECHNOLOGY

NOVEMBER/DECEMBER 2001

The Journal of Gear Manufacturing

FEATURES

43

DEPARTMENTS

56

Cover art courtesy of Bodine Electric Co., Chicago, IL.

GEAR TECHNOLOGY

The Journal of Gear Manufacturing

EDITORIAL

Publisher & Editor-in-Chief Michael Goldstein

Managing Editor William R. Stott

Associate Editor Joseph L. Hazelton

Editorial Consultant Paul R. Goldstein

Technical Editors
Robert Errichello
Don McVittie
Robert E. Smith
Dan Thurman

ART

Art Director Jean Bartz

ADVERTISING

Advertising Manager Patricia Flam

CIRCULATION

Circulation Coordinator Dina Krauss

INTERNET

Web Developer Dan MacKenzie

***Gear Industry Home Page*™ Sales**
Patricia Flam
David Tomalis

***powertransmission.com*™ Sales**
Emily C. Frankenberger

RANDALL PUBLISHING STAFF

President Michael Goldstein
Vice President Richard Goldstein
Controller Michael Grafman
Accounting Dianne Johnson

Phone: 847-437-6604
E-mail: ***people@geartechnology.com***
Web: ***www.geartechnology.com***
www.powertransmission.com

BPA INTERNATIONAL

VOL. 18, NO. 6

GEAR TECHNOLOGY, The Journal of Gear Manufacturing (ISSN 0743-6858) is published bimonthly by Randall Publishing, Inc., 1425 Lunt Avenue, P.O. Box 1426, Elk Grove Village, IL 60007, (847) 437-6604. Cover price $5.00 U.S. Periodical postage paid at Arlington Heights, IL, and at additional mailing office. Randall Publishing makes every effort to ensure that the processes described in GEAR TECHNOLOGY conform to sound engineering practice. Neither the authors nor the publisher can be held responsible for injuries sustained while following the procedures described. Postmaster: Send address changes to GEAR TECHNOLOGY, The Journal of Gear Manufacturing, 1425 Lunt Avenue, P.O. Box 1426, Elk Grove Village, IL, 60007.

With Forest City Gear
You've Landed the
Best Gears Possible!
Stop Fishing for a Gear Manufacturer
Forest City Gear offers World Class Gear Quality
NEW: Gear & Thread Grinding
• Crown hobbing for noise reduction and misalignment compensation.
• Hard hobbing with carbide hobs after heat treat as a substitute for gear grinding.
• CNC hobbing and shaping alignment programs for varying teeth and pitches.
• Hobbing 2 tooth & greater helical pinions.
• Special forms, high helix worms and camshafts.
• Precision analytical gear inspection.
• Hob sharpening.
Forest City Gear...the most modern fine and medium pitch gear job shop in the world.
815-623-2168
Fax: 815-623-6620
Toll Free: 866-623-2168
11715 Main Street
P. O. Box 80
Roscoe, IL 61073-0080
We welcome our competitors!
www.fcgear.com
ISO 9002 Registered
PRO
Member of the American Gear Manufacturers Association
FOREST CITY GEAR
W.F. Kickapoo Avalanche, Wisconsin

CIRCLE 138

Who Makes the Nails?

For want of a nail the shoe was lost.
For want of a shoe the horse was lost.
For want of a horse the rider was lost
For want of a rider the battle was lost.
For want of a battle the kingdom was lost.
And all for the want of a horseshoe nail.
—Nursery Rhyme

I've been thinking a lot about the importance of manufacturing over the last couple of years, especially as I've watched more and more of it leave our country. We work in an industry that is both economically and strategically vital, but I'm concerned that most Americans do not realize the importance of manufacturing, or what will happen if it continues to dissipate.

It used to be that we made everything we needed here in America. We don't anymore. For example, one of my employees recently bought an American flag. Imprinted on the flag in tiny letters were the words "MADE IN CHINA." Although the importance of manufacturing U.S. flags is more symbolic than strategic or economic, it still makes me wonder. If somebody else is manufacturing our own flag, what else are they manufacturing?

I spoke recently with an American gear manufacturer whose business is mostly aerospace- and defense-related. A while back, he lost some important gear business to a company in Eastern Europe. As it turns out, he got most of the business back because his customer was unhappy with the overseas results. This American gear manufacturer's business is up 34% over last year. I'm comforted by the fact that in this case, some crucial manufacturing capability has remained in America. But at the same time, I'm disturbed by the fact that it almost didn't.

The recent terrorist attacks on the World Trade Center and the Pentagon have pointed out the significance of our manufacturing capabilities. We need manufactured goods to respond to emergencies, rebuild what's broken and defend our nation. We need rescue equipment, construction equipment, vehicles and much more to clear away the rubble and rebuild. We need all sorts of sophisticated equipment to defend our country from further attacks.

During World War II, many factories were taken over by the government and retooled for wartime production. Then, machine tool manufacturers were told what to build and where to ship it for our defense efforts. Today, there are hardly any machine tool manufacturers left in America. Will we come to the point when we are unable to make the parts we need for our country's aircraft, tanks, missiles and other defense-related machines? Probably not, but in an extended crisis, we could easily find ourselves unable to produce what we need.

Even in times of peace, manufacturing is vital. Most people outside manufacturing don't realize how important it is to the economic well-being of a nation. Manufacturing is the creation of wealth. Manufacturers take raw materials, and by performing various processes, create something of greater value.

In addition to creating wealth, the manufacturing industries have always provided a lot of challenging, satisfying, necessary and good-paying jobs for America.

Of course, I'm not telling you anything you don't already know. You are all involved in manufacturing every day. I'm confident that, like me, you're proud to be involved in an industry that contributes so much to our nation's well-being. It would be nice, however, if the rest of America could see what we see.

I am entirely optimistic that this nation can overcome whatever challenges come its way. After all, we still operate the world's largest manufacturing economy. We make a tremendous variety of goods, and our technological capabilities continue to improve, year after year. But when things return to normal, will we forget the lessons we've learned? I hope not, because we can't afford to wait for the next crisis—strategic or economic—to find out if we'll be able to respond.

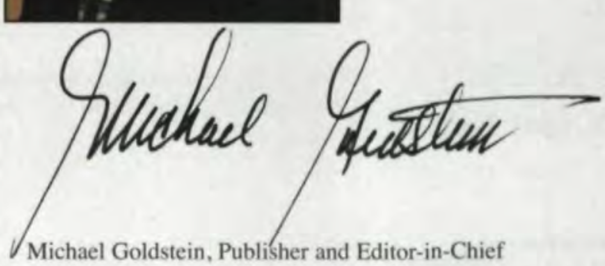

Michael Goldstein, Publisher and Editor-in-Chief


powered by SAMPUTENSILI

Laser Shock Peening

Bombarding metal parts with tiny metal or ceramic beads seems like a crazy way to improve those parts' performance, but shot peening is a proven method of improving the fatigue life of metal parts, especially those that are prone to surface fatigue failures. Now, there's an even more unusual tool—lasers—to perform the same function, only better.

Laser peening can extend the service life of some parts, including gears. The extension of service life can be anywhere from 3–10 times the extension given by normal shot peening, according to industry experts, because laser peening puts compressive stress much deeper into the part.

The concept of using lasers to introduce residual stresses into a part's surface of a part was invented at Battelle of Columbus, OH, in the late 1960s and early 1970s. But it really didn't become practical for production use until the late 1990s, as the technology improved and commercial companies began to develop it.

One of those companies, LSP Technologies Inc. of Dublin, OH, was founded in 1995 by former Battelle employees and has done work for the U.S. Air Force. Another company, Metal Improvement Co. Inc. of Paramus, NJ, has worked with Lawrence Livermore National Laboratory of Livermore, CA, to develop laser peening.

"We think that laser peening, based on recent advances, is a technology that is going to see widespread use," says Lawrence Livermore physicist Lloyd Hackel.

Metal Improvement Co. is developing laser-peened gears for engine transmissions. According to James Daly, senior vice president of the company, construction, mining, farming, marine and over-the-road tractor truck transmission components are being required to have their guaranteed service lives extended.

"One or a few problem gears can represent a lifetime limitation," Daly says. But laser peening those gears could extend the lifetime of the entire transmission and be a very cost-effective step in quality improvement.

LSP Technologies is also working extensively with gears, including ring and pinion sets and other automotive drivetrain gears, says president Jeff Dulaney.

Laser peening is more effective than shot peening, and it's beginning to be used on gears, including this automotive ring and pinion set processed by LSP Technologies Inc.

How it Works

When most people think of lasers, they think of them as a tool for cutting through metal, but that's not how laser peening works. In fact, light from the lasers never touches and never heats the part surface. Instead, the lasers are used to generate a shock wave that causes compression at the part surface.

The part to be laser peened is coated with an opaque, absorptive material—a special paint or tape that will vaporize when exposed to a pulse of laser energy. The part is also covered with a thin layer of translucent material, which is usually water. A pulsed laser beam passes through the water and strikes the paint or tape, causing a small thickness of the material to vaporize. The vapor absorbs the remaining laser light, creating plasma, which is trapped in a small gap between the absorption material and the water layer. The trapped plasma builds to a pressure of up to 100,000 atmospheres (about 1.5 million pounds per square inch) and creates a compressive shock wave, part of which runs into the metal surface.

A pulsed laser beam creates a shock wave that causes beneficial compressive stresses in the roots of these gear teeth. Photo courtesy of Metal Improvement Co. Inc.

Welcome to* Revolutions, *the column that brings you the latest, most up-to-date and easy-to-read information about the people and technology of the gear industry.* Revolutions *welcomes your submissions. Please send them to* Gear Technology, *P.O. Box 1426, Elk Grove Village, IL 60009, fax (847) 437-6618 or e-mail* people@geartechnology.com. *If you'd like more information about any of the articles that appear, please circle the appropriate number on the Reader Response Card.

That part of the shock wave causes plastic deformation of the part surface, leaving compressive residual stresses that prevent cracks from growing and thus improve the part's fatigue life.

According to Dulaney, the LSP Technologies laser-peening process creates compressive stresses at depths ranging from 0.040" to 0.060". According to Daly, Metal Improvement Company's laser peening creates compressive stresses to depths of 0.040" to 0.080". In both cases, the compressive stresses are significantly deeper than through shot peening. This extra depth provides even greater protection against surface-related failures, such as fatigue cracks and corrosion cracking.

Laser peening can be used in conjunction with normal shot peening, Dulaney says. An entire part is typically shot-peened, and then the areas of high stress concentration, which are prone to fatigue cracking, are further treated with laser peening. Those areas include the roots of gears, says Hackel.

Applicability

Because laser peening is more expensive and takes longer than normal shot peening, it's been used mostly for expensive, highly critical parts. One of the biggest applications to date has been the laser peening of the leading edges of the blades of aircraft turbines. Normally, these parts are shot-peened to improve their performance. Laser peening increases the performance even further. According to Dulaney, that increased performance amounts to savings of millions of dollars per year for the U.S. Air Force.

Both the cost of laser peening and the amount of time it takes are decreasing, which should open the applicability of the process to many more parts, says Daly.

In addition to aerospace turbines and gears, the organizations involved in this technology have begun targeting products as diverse as oil drilling equipment; medical implants, such as hip joints; marine and rocket engine parts; automotive crankshafts and connecting rods; and tooling and dies.

Circle 300

A New Heat-Treating Process

A new heat-treating process could harden internal gear teeth using a lamp that can radiate 3,500 Watts per square centimeter, with a brightness that rivals the sun's.

The lamp could harden internal gear teeth by being slid into and pulled out of a gear's opening.

The high-intensity plasma arc lamp consists of a cathode, an anode, a clear quartz tube, argon gas and deionized water. The lamp's power is generated by circulating the gas and water through the tube, from the cathode to the anode, around the electric arc between those two electrodes.

The water is pushed against the tube's inner walls while the gas is ionized along the centerline. The gas then emits large amounts of radiant energy, which pass through the water and quartz.

The process is being developed by Vortek Industries Ltd. of Vancouver, Canada, and Oak Ridge National Laboratory, located in Oak Ridge, TN.

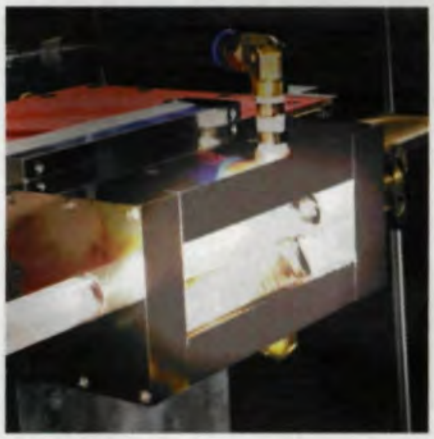

Capable of radiating 3.5 kW/cm², Oak Ridge National Laboratory's plasma arc lamp glows brilliantly as it hardens steel without hardening the entire workpiece. The lamp's hardening ability could be used on internal gear teeth.

At Oak Ridge, Craig Blue is the technical lead in the Infrared Processing Center, in the laboratory's Metal & Ceramics Division. He holds a doctorate in materials science, with a specialty in radiant/infrared processing of materials.

"We can get full hardness in our material," Blue says. "We can harden steel at up to a meter per minute."

The lamp can run from 2% to 100% of its radiant output and can continuously vary that output, changing the power level in less than 20 milliseconds. Thus, the lamp can compensate for different thicknesses of metal and thereby provide a constant case hardness.

Such radiant heating has very high heat transfer efficiences because there's no intermediate material to absorb heat between the lamp and the workpiece.

Also, radiant heating can be precisely controlled and isn't affected by processing atmospheres.

Blue's processing facility has been operable since spring 1999 and consists of the high-intensity plasma arc lamp, an industrial robot and PC-based controls.

The lamp was invented about 29 years ago by Vortek Industries.

"Up until about the last three years, it had very limited use," Blue says of the lamp. "Because of its relatively short life." He explains that the life was measured in hours.

But, according to Blue, Vortek extended the lamp's life to hundreds of hours by further developing the lamp's anode and cathode.

The cost is $300,000 for the machinery, with a 300,000 Watt lamp. Blue says the cost is similar to induction heat treating.

Since it became operable, Blue has tested his process to determine possible applications, including heat treatment of flat-stock powder metal parts.

But, he hasn't used his process on gears, so he has no data about heat-treating them. But, he does have data about heat-treating steel, and gears are steel.

"Then you're just talking about geometry," Blue says.

Besides not developing his process for gears, he also hasn't talked to anyone about developing it for gears.

If a gear manufacturer came to him, though, Blue says he might develop his process for gears. Also, the laboratory has programs for working with commercial organizations to develop processes they need.

Blue estimates it would take a year to develop his process to heat-treat gears.

Circle 301

Tell Us What You Think . . .

If you found this column of interest and/or useful, please **circle 321.**

If you did not care for this column, **circle 322.**

Dry Machining for Gear Shaping

Jürgen Schmidt, Oliver Doerfel and Andreas Hühsam

This paper was originally presented at the 4th World Congress on Gearing and Power Transmission in Paris, March, 1999.

Introduction

Economic production is one of the main concerns of any manufacturing facility. In recent years, cost increases and tougher statutory requirements have increasingly made cutting fluids a problematic manufacturing and cost factor in metalworking. Depending on the cutting fluid, production process and supply unit, cutting-fluid costs may account for up to 16% of workpiece cost. In some cases, they exceed tool cost by many times (Ref. 1). The response by manufacturers is to demand techniques for dry machining (Ref. 2).

Fundamentals of Cutting Kinematics

Gear shaping is one of the continuous generating processes in metal-cutting gear manufacture. The arrangement of cutter and workpiece during the shaping process corresponds to the configuration of a spur gear pair, with three movements (Ref. 3):

- Cutting movement of tool,
- Rotary movement of cutter and workpiece, and
- Radial movement of cutter.

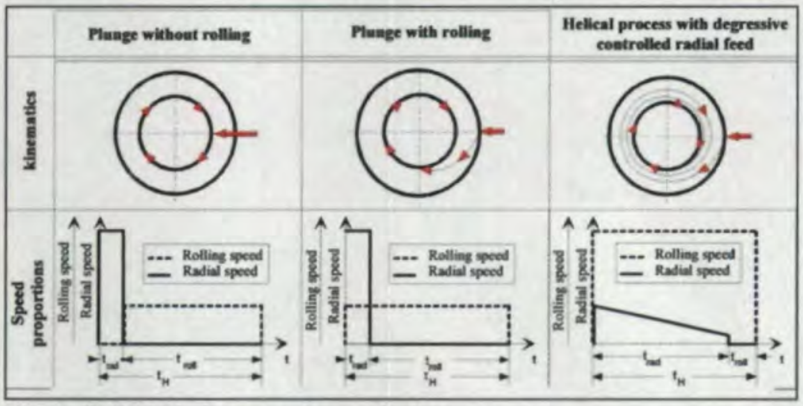

Fig. 1—Radial in-feed processes in gear shaping.

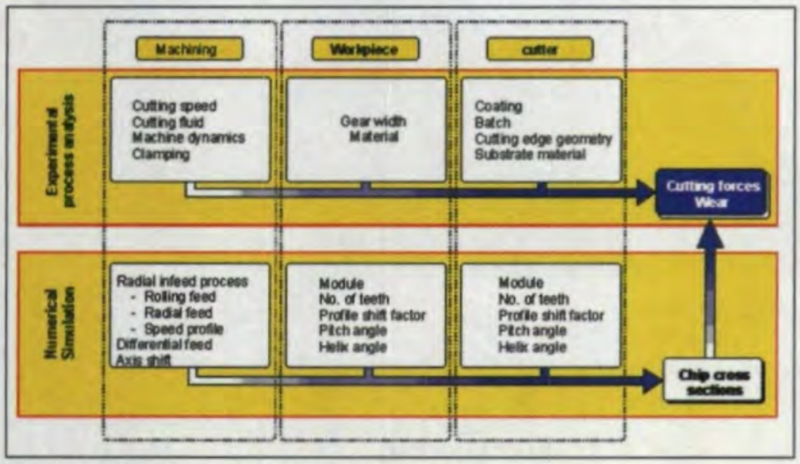

Fig. 2—Main parameters in gear shaping/approach.

Basically, there are three in-feed processes that may be distinguished by radial movement (Fig. 1) (Ref. 4):

Plunging without rolling movement. In plunging without rolling, radial in-feed is effected without a rotation movement of tool and workpiece. Radial feed remains constant throughout in-feed. After the in-feed depth has been reached, the gear is rolled out once at tooth depth, whereby the rolling feed is relatively low, due to the large overlap of tool and workpiece.

Plunging with rolling movement. In plunging with a rolling movement, the in-feed rate of the tool and the in-feed depth are achieved with simultaneous turning of the tool and the workpiece, whereby the rolling angle covered is usually less than 180°. Similar to plunging without rolling, this process causes the teeth to be rolled out to in-feed depth.

The radial in-feed processes of plunging with and without rolling are among the "conventional" in-feed processes and are comparable in terms of their characteristics. The radial and rolling feeds are similar.

Helical process with degressive-control radial feed. The in-feed rate and in-feed depth in the helical process with degressive-control radial feed is effected continuously over a number of workpiece revolutions. The speed of radial feed decreases over the rolling path, i.e. at the beginning of machining, radial feed rate is high, and it decreases with increasing overlap of workpiece and tool. That results in a linear relationship between radial feed rate and time. The current rolling feeds are higher by a factor of two or three compared with plunging with or without rolling, with comparable main production times. That is due to the lower amounts of radial feed.

The advantage of the helical in-feed process compared with the processes mentioned above is that there is homogeneous tool load over the entire machining process. It is known that helical degressive radial in-feed causes cratering wear of the tool face, while conventional radial in-feed processes (plunging with or without rolling) cause flank wear. The causes and optimization strategies are presented in the numerical simulation.

Approach

The aim here was to find a universally applicable way of eliminating cutting fluids in gear shaping processes. A two-part process has therefore been specified, based on the main process parameters (Fig. 2). There are two main sets of parameters that influence wear and cutting forces. One set includes geometry-dependent parameters that directly affect chip cross section, which influences cutting forces and cutter wear. The other set includes parameters that have a direct impact on cutting forces and wear, without any change in the chip cross sections. Both sets of parameters can be broken down into machining, cutter and workpiece parameters. In order to achieve comprehensive optimization of gear shaping, it is necessary to consider both the chip cross sections and the technological parameters.

Keeping chip cross section constant, an experimental process analysis was conducted to analyze the influence of technological parameters on wear behavior and cutting forces. A numerical simulation was done to systematically analyze the cutting process by a geometry-related model, to determine and optimize the chip cross sections. The results were used to obtain assessment criteria for chip cross sections, and the model presentation was then verified in experiments.

Experimental Process Analysis

The aim of the experimental process analysis was to characterize the influence of various technology parameters while maintaining constant chip cross section. Cutting force measurements were used to analyze the loads occurring on the cutter under different machining conditions, in order to understand the process as a whole. The resulting wear analysis was then used to determine form and wear amount, so the knowledge could be used to improve coatings and optimize cutter life in dry machining.

Cutting force measurements to optimize technological data. Cutting force measurements were used to analyze the influence of manufacturing conditions on cutter load, both in the radial in-feed techniques (plunging with and without rolling) and in gear cutting with degressive radial feed. The comparison was based on equal main production times. The analysis showed that, depending on the

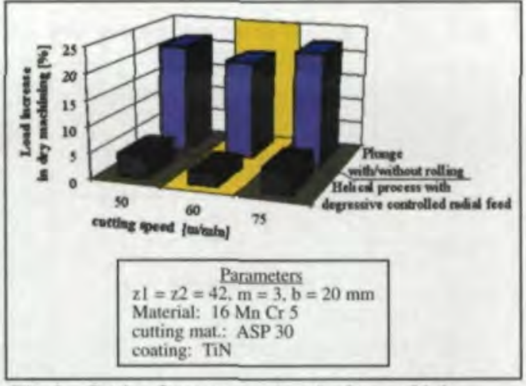

Fig. 3—Cutting force comparison in dry machining.

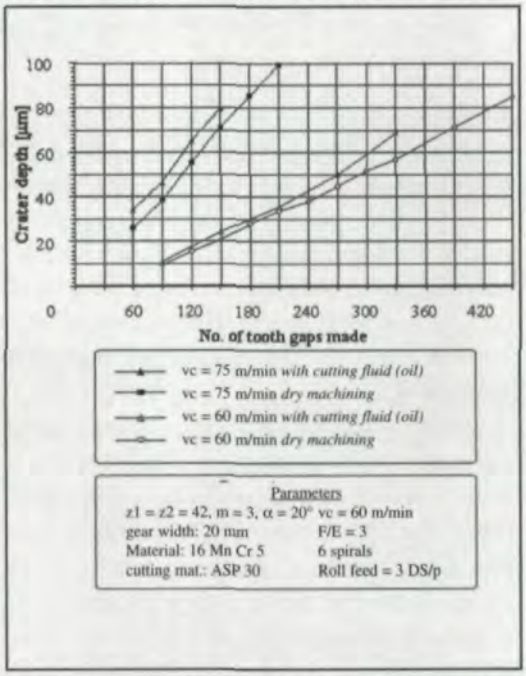

Fig. 4—Influence of cutting fluid and cutting speed on crater depth.

gear cutting process, dry machining increases cutter load by up to 25% (Figure 3).

In conventional gear cutting processes (plunge with or without rolling), the load increase in dry machining is between 15% and 25%, depending on the cutting parameters used (shown with the example of cutting speed). In helical degressive radial in-feed, the omission of cutting fluid means that increase in cutting speed causes considerably less increase in main cutting force (about 5%). That is due to the high rolling feeds, with only short contact times between the tool and the chip. Also, the proportion of frictional work in chip formation is small. The "lubricating" function of the cutting fluid only plays a minor part under those contact conditions. The cutting force measurements show that the helical degressive radial in-feed technique is more suitable for dry machining than the conventional in-feed processes. That technique is therefore used in the subsequent investigations.

Tool life analysis in dry machining. The pur-

Prof. Dr.-Ing. Jürgen Schmidt

is speaker of the common board of leadership at the Chair and Institute of Machine Tools and Production Science, University of Karlsruhe, located in Germany. A mechanical engineer, he also is sponsor of the institute's manufacturing technology group.

Dr.-Ing. Oliver Doerfel

works for DaimlerChrysler AG. A mechanical engineer, he heads a team of mechanical engineers that plan production concepts and systems for material flow. Previously, he was a scientific employee at the Chair and Institute of Machine Tools and Production Science, where he earned his doctorate in 1998 on gear shaping.

Dipl.-Ing. Andreas Hühsam

is a scientific employee in the manufacturing technology group of the Chair and Institute of Machine Tools and Production Science. A mechanical engineer, he works on developing innovative manufacturing procedures for gearing, especially gear skiving.

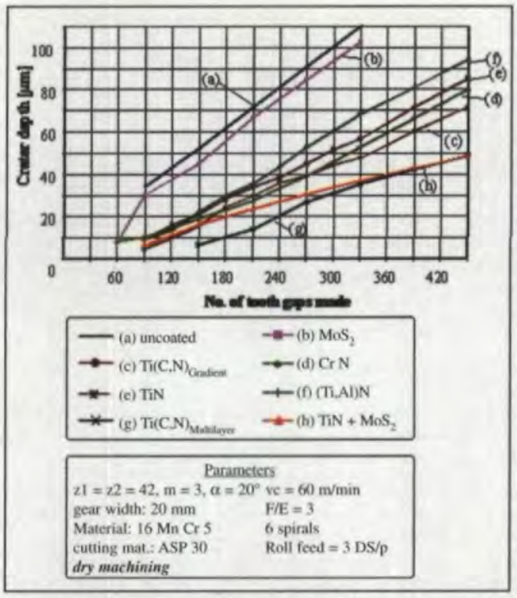

Fig. 5—Influence of coating on cutter life in dry machining (Ref. 6).

pose of the tool life analysis was to determine the effect of cutting fluid and cutting speed on tool life and workpiece quality. Further analysis was conducted to show the potential of innovative tool coatings.

Figure 4 shows the influence of cutting speed and cutting fluid on crater depth, using the example of tools coated with standard titanium nitride (TiN). The figure shows that an increase of cutting speed from 60 m/min. to 75 m/min. (25%) increases crater depth, regardless of lubrication conditions. Extrapolating the values to a crater depth of 100 µm, cutting speed increase reduces tool life to 30% of the original level.

It is also clear that, for the same cutting speed, there is very little difference between tool life achieved in dry machining and conventional cutting fluid application. For a specified tool life, dry machining always gives less crater depth than wet machining. The higher temperature of the chip and the related shorter chip path also reduce crater lip distances in dry machining. But, there is no premature breaking of the crater lip in dry machining.

Influence of coating. Recent developments in coating technology have given major benefits in cutter wear resistance (Ref. 5). Firstly, production processes for coating manufacture have been optimized. Secondly, new layer systems have been developed and adapted to specific production processes. With that background in mind, innovative layer systems have been examined to determine suitability for the specific requirements of the gear shaping process. The aim of the experimental study was to achieve a major increase in cutter life.

Apart from the commercially standard hard layers—like chromium nitride (CrN), titanium aluminium nitride ((Ti,Al)N) and titanium carbonitride gradient (Ti(C,N)$_{gradient}$)—the following new types of coating also were applied to the tools and tested in experimental trials to determine possible increase in performance in gear shaping:

Ti(C,N) multilayer coating. The titanium carbonitride multilayer coating was applied by an optimized process. That involved frequent alternation of TiN and Ti(C,N) layers in the multilayer deposit, with standard layer thicknesses (3µm) to achieve low inherent stress. That resulted in improved adhesion combined with good microhardness, compared with the standard Ti(C,N) gradient coatings (just one continuous transition from TiN to Ti(C,N)).

Solid lubricant layer (MoS_2). The solid lubricant layer molybdenum disulfide (MoS_2) on the cutting wedge was intended to replace the cutting fluid's "lubrication" function. The solid lubricant layer featured a very low friction coefficient (μ = 0.04–0.09 with steel). The coating was applied in a sputter process at low coating temperatures.

Hard coating layer + solid lubricant layer (TiN+MoS_2). This system separated the functions at the cutting layer, with suitable combination of a hard layer (e.g. TiN) as a base coating on the substrate and a solid lubricant layer (MoS_2) additionally applied to the hard coating. The hard coating improved the wear behavior of the tool, while the solid lubricant layer reduced friction between chip and tool.

Figure 5 shows the effect of the layers described above on cutter life in dry machining. A comparison with uncoated tools shows that a hard coating (e.g. TiN) always has a positive impact on tool life.

For identical cutting conditions, the different standard coatings—Ti(C,N)$_{gradient}$, (Ti,Al)N, TiN and CrN—resulted in only minor differences in tool life. There was only slight difference in crater depths between these tools for a tool life of 450 tooth gaps cut. The tools sputtered with MoS_2 had very unfavorable tool life. Wear investigations showed that the MoS_2 layer was no longer present after cutting just a few tooth gaps. Further wear depended on the substrate core, and the wear characteristic was almost identical to that of uncoated tools.

The use of TiN+MoS_2 coated tools gave quite different results, with very favorable tool life. Direct comparison with the standard coatings showed that for 450 tooth gaps cut, the crater depth was only half as great. Visual assessment of this coating system showed that, here again, the MoS_2 layer was no longer present after cutting just a few tooth gaps. The solid lubricant was present in the surface structure of the TiN layer, as shown by metallographic examinations. A combination of hard material and solid lubricant layer gave double the tool life on extrapolation of the wear curves.

A good wear characteristic similar to the "combined layer" TiN+MoS_2 also was given by the Ti(C,N) multilayer coated tools. The improvement in coating methods means that dry machining, like the TiN+MoS_2 layer, gives double the tool life compared with standard layers.

Numerical Simulation of Chip Cross Sections

The superposition of the three main movements combined with the three-cutting-edge tool gives a wide range of chip cross sections in gear shaping. To improve the dry machining of a workpiece, the chip cross sections have to be varied, and optimized with a defined target magnitude. Purely experimental adjustment of chip cross sections to each specific application involves a great deal of effort. Experimental optimization of chip cross sections means a lot of work for each customer-specific gear design and is not always an appropriate method.

The complexity of the situation makes it essential to use computer-aided optimization of chip cross sections, based on analysis of the relationship between workpiece and tool geometry and the machining parameters. A simulation program has been created to permit personal-computer-based modelling of the chip cross sections, using a systematic and universal program structure. The simulation is based on knowledge of the existing tool geometry and of the exact movement equations, dependent on in-feed method. The chip cross sections can be shown by coupling the geometry of the tool with the movement equations of the gear shaping process, and the cut with the respective workpiece contour, whereby the kinematics of the gear shaping process are shown by coordinate transformation between different reference coordinate systems. That coupling gives the chip cross sections of the process and the derived chip attributes. Chip cross sections are determined for a given workpiece/tool geometry and for specified machining parameters, and evaluation is done on the basis of chip attributes (e.g. area, maximum chip thickness) and chip shape.

Comparison of in-feed processes. Figure 6 shows the major chip attributes of the radial in-feed processes (plunging with or without rolling),

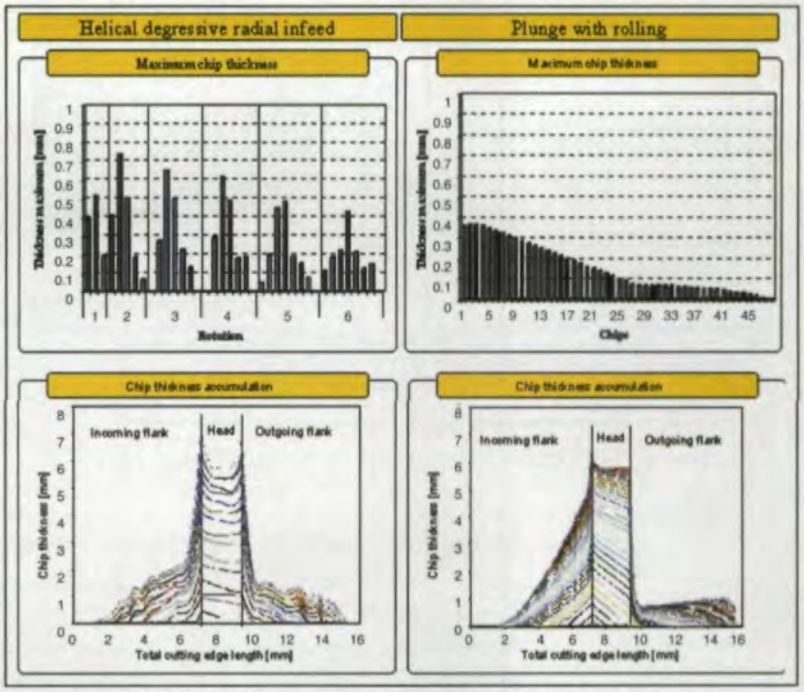

Fig. 6—Comparison of chip cross section for various in-feed processes.

and helical degressive radial in-feed. For plunging with rolling, one tool tooth is considered, rolling into the workpiece at in-feed depth. Comparison of the characteristic of maximum chip thickness shows that plunging with rolling gives the values for chip thickness maxima that are several times lower than for helical degressive in-feed. That is because the rolling feed in the process is smaller by a factor of three or four. Helical degressive in-feed gives only a small amount of radial feed in the individual rotations, and yet maximum chip thicknesses are still very great. That means that the division of in-feed depth over a number of machining rotations has only minor influence on maximum chip thickness.

According to Victor (Ref. 7), the chip thickness (alongside chip width and specific cutting force) is a major parameter for the amplitude of the cutting force, and thus has a direct influence on tool wear. For every individual chip cross section, it is possible to analyze the characteristic of chip thickness along the developed absolute cutting edge length of the tool. The large number of chip thicknesses in the manufacture of a gear produces a whole host of information, too much to analyze. A cumulative presentation of chip thicknesses is therefore used here, described as chip thickness total, the total cutting edge load occurring at the various tool cutting edges. The characteristic of chip thickness total for one cutter tooth is obtained by adding the respective chip thickness characteristics of each chip cross section. The distance between two characteristics in

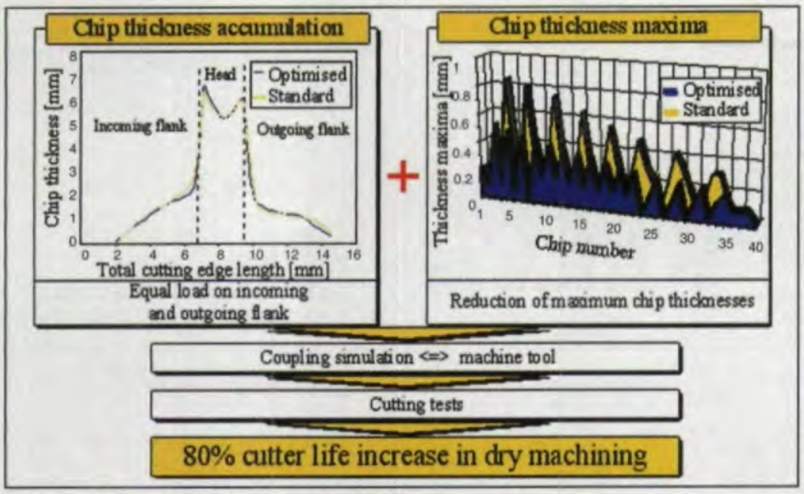

Fig. 7—Optimization of chip cross sections.

Figure 6 thus shows the chip thickness for one chip.

Comparison of the calculated chip thickness totals shows very clearly why plunging with rolling gives wear on the flank at the transition zone from the tooth head to the end of the flank. The low gear shaping feed means that the major part of the workpiece gap is cut by the incoming flank and the tooth head. In the transition zone between tooth head and end of flank, the overall result is only very thin chips, which cause frictional wear on the flank. Due to the small amount of rolling feed, that wear is not caused by chip formation, but can be attributed to the crushing of thin chips. The overall cutting edge load for helical degressive radial in-feed is characterized by uniform loading of incoming and outgoing flank, which causes crater wear development without wear of the flank.

A comparison of the in-feed processes shows a strategy for definition of goals to optimize in-feed parameters:

• Uniform loading of incoming and outgoing flank areas to achieve crater wear on the tool,

• Reduction of maximum chip thickness to reduce wear on the assumption of "crater wear formation," and

• Avoidance of very thin chips.

Optimization of chip cross sections. The major technological data of helical degressive radial in-feed were varied with the goal of crater wear formation and thus constant tool quality during cutter life.

Figure 7 shows the aggregated chip thickness and the resulting maximum chip thicknesses for a standard technology data set, and an optimized data set, in comparison. Uniform loading of incoming tool flank and outgoing tool flank gives crater wear of the tools (compare chip thickness aggregation). Compared with standard machining cases, this optimized data set considerably reduces maximum chip thicknesses. Validation in the cutting test shows that optimization of technology data can increase cutter life by 80%. This shows just what potential there is in optimizing chip cross sections. In order to improve wear form and wear amount, it therefore makes sense to conduct a computer-aided analysis of chip cross sections in advance, in the course of production planning.

Summary

Dry machining is currently one of the most widely discussed subjects in metal cutting, due to issues of ecology, economics and industrial health and safety.

A two-part approach has been chosen, derived from the main parameters of the gear shaping process. Experimental investigations showed that optimization of cutting conditions will already permit dry machining with conventional coatings. Targeted improvement of the layer made it possible to double tool life. Numerical simulation of chip cross sections can be used to analyze wear form and nearly halve tool wear.

The two-part approach used here makes it possible to adapt a wide range of workpiece geometries to the changed parameters of dry machining. Further investigation will be required to determine how far existing machine tool concepts are suitable for dry machining. ○

References

1. Klocke, F. and G. Eisenblätter, "Dry Cutting," *Anals. of CIRP*, Vol. 46/2/1997.
2. Tönshoff, H. K. "Reducing Use of Coolants in Cutting Processes," *Production Engineering*, Vol. I/2, 1994.
3. Sulzer, G. *Leistungssteigerung bei der Zylinderherstellung durch genaue Erfassung der Zerspankinematik*, Dissertation TH Aachen, 1973.
4. Thämer, R. "Moderne Verzahnungstechnik des Wälzstoßens," *Die Maschine*, Seite 26-289/, 1984.
5. Anklam, H-J, "Abscheidung von Hartstoffschichten mittels Arc-Verdampfens'," Seminar Oberflächenbehandlung mit Plasmen, 2.Teil Beschichtung, November 1993, Essen.
6. Schmidt, J. and O. Doerfel, "Zahnräder wälzstoßen ohne Kühlschmierstoff," *Maschinenmarkt 103*, Nr. 29, S. 26-29, 1997.
7. Victor, H. *Beitrag zur Kenntnis der Schnittkräfte beim Drehen, Hobeln und Bohren*, Dissertation Universität Hannover, 1956.

Tell Us What You Think . . .

If you found this article of interest and/or useful, please **circle 319.**

If you did not care for this article, **circle 320.**

If you would like to respond to this or any other article in this edition of *Gear Technology*, please fax your response to the attention of Randy Stott, managing editor, at 847-437-6618.

TECHNICAL CALENDAR

Nov. 7—Gear Measurement Codes of Practice. The Riverside Hotel, Burton on Trent, England. Learn the codes of practice used by a number of United Kingdom companies for gear measurement. The codes cover gear measurement from drawing specification through routine inspection to machine calibration. For more information, visit the British Gear Association's website at *www.bga.org.uk*.

Nov. 13–16—PTC China 2001: Leading Exhibition for Power Transmission and Control, Fluid Power, Internal Combustion Engines and Gas Turbines. Shanghai New International Expo Center, Pudong, China. The trade fair features basic machinery components, including loose gears, speed reducers and other gear units. Besides mechanical power transmission, other types of exhibits are expected to include electrical power transmission, internal combustion engines and small gas turbines, and motion control technology and products. For more information, contact one of the following people. For China, Hong Kong and Taiwan, contact Judy Zhu of Hannover Fairs China Ltd.–Shanghai by telephone at (86) 21-6886-3286 or by e-mail at *shanghai@hfchina.com*. For Europe and the United States, contact Carsten Fricke of Deutsche Messe AG by telephone at (49) 511-89-32-113 or by e-mail at *carsten.fricke@messe.de*.

Nov. 15–17—JSME International Conference on Motion and Power Transmissions. ACROS Fukuoka, Fukuoka, Japan. Technical papers presented will cover a variety of gear-related topics. Conference includes forum on future of gears in the 21st century. Conference's official language is English. Papers should be written and presented in English. Sponsored by the machine design and tribology division of the Japan Society of Mechanical Engineers. For more information, contact the conference secretariat by sending e-mail messages to *secretariat@MPT2001.mech.kyushu-u.ac.jp*.

Nov. 20—Steels Day. Corus Engineering Steels, Rotherham, England. The seminar is meant to provide gear designers and manufacturers with the latest information on the production and properties of modern engineered steels. The seminar will cover secondary steelmaking and continuous casting, cleanness and composition control, and improved machinability. For more information, visit the British Gear Association's website at *www.bga.org.uk*.

Tell Us What You Think . . .
If you found this column of interest and/or useful, please **circle 323**.

If you did not care for this column, **circle 324**.

If you would like to respond to this or any other article in this edition of *Gear Technology*, please fax your response to the attention of Randy Stott, managing editor, at 847-437-6618 or send e-mail messages to *people@geartechnology.com*.

Profile Shift in External Parallel-Axis Cylindrical Involute Gears

Phillips D. Rockwell

Introduction

Early in the practice of involute gearing, virtually all gears were made with the teeth in a standard relationship to the reference pitch circle. This has the advantages that any two gears of the same pitch, helix angle and pressure angle can operate together, and that geometry calculations are relatively simple. It was soon realized, though, that there are greater advantages to be gained by modifying the relationship of the teeth to the reference pitch circle. The modifications are called profile shift. Advantages include:

1. Ability to balance bending fatigue life of pinion and gear.
2. Ability to balance specific sliding on either side of the pitch point. Balanced specific sliding maximizes pitting resistance.
3. Ability to balance (and therefore minimize) peak contact flash temperatures on either side of the pitch point. This minimizes the probability of scuffing.
4. Ability to avoid or reduce undercut on pinions with small numbers of teeth.

Item 4 will generally not be necessary unless there is something special about the application that requires a small number of teeth. Normally, in good gear design practice, pinions that have a tooth number approaching the minimum to avoid undercut are not used—they have large teeth, high specific sliding, and are prone to scuffing failure (Ref. 4, p. 12). Unless there are special requirements for the application, optimal design usually will give a number of pinion teeth well above the minimum to avoid undercut. The algorithm presented in this article does not attempt to determine optimum tooth numbers. For a procedure to determine optimum pinion tooth numbers, see Reference 4.

Gears with profile shift can be made with the same methods and tooling as standard gears, namely hobbing or shaping with rack cutters or pinion cutters. This article deals only with rack cutters and hobs. (The parameters for rack cutters are the same as those for hobs.)

There is some confusion in the gear engineering community regarding profile shift, particularly with regard to the need for tip shortening and the size of generated root circles. This article will clarify some of the issues that may be causing confusion, and it will give an algorithm for deriving tip radii and other parameters after certain parameters have first been established.

Europeans have established consistent gear terminology and symbols, so in this article—for the most part—European gear terminology and symbols will be used. See Tables 1, 2 and 3.

Table 1—Symbols

Symbol	Units	Description
a	mm or inches	Operating center distance—the actual center distance at which the gears are mounted.
a_d	mm or inches	Reference center distance—the center distance the gears would be mounted at if they were standard gears.
c_{12}	mm or inches	Pinion tip clearance—the distance from the pinion tip circle to the gear root circle, measured along the line of centers.
c_{21}	mm or inches	Gear tip clearance—the distance from the gear tip circle to the pinion root circle, measured along the line of centers.
f_n	—	Total normal finish allowance per side, normalized.
f_{no}	—	Normal finish allowance per side built into tool, normalized.
h_a	mm or inches	Addendum—the radial distance from the reference pitch circle to the tip circle.
h_{a01}	—	Pinion tool addendum—the distance from the tool reference line to the tips of the tool teeth, normalized.
h_{a02}	—	Gear tool addendum—the distance from the tool reference line to the tips of the tool teeth, normalized.
inv	—	Involute function—takes radians as argument.
j_n	—	Normal operating circular backlash, normalized.
k	—	Tip shortening coefficient, normalized.
m_n	mm or inches	Normal module.
p_N	mm or inches	Normal base pitch.
p_b	mm or inches	Transverse base pitch.
r	mm or inches	Reference pitch radius.
r_w	mm or inches	Operating pitch radius.
r_a	mm or inches	Tip radius.
r_b	mm or inches	Base radius.
r_f	mm or inches	Root radius.
s	mm or inches	Circular tooth thickness.
Δs_n	—	Normal tooth thinning for backlash at reference radius, normalized.
u	—	Gear ratio.
x_1 (x_2)	—	Pinion (gear) profile shift coefficients.
x_{g1} (x_{g2})	—	Pinion (gear) rack shift coefficients.
z_1 (z_2)	—	Pinion (gear) number of teeth.
α	—	Pressure angle.
β	—	Helix angle.

Influence of Profile Shift

For a given normal module, normal pressure angle, reference helix angle and number of teeth, the base circle radius does not change, regardless of whether the gear has profile shift. Since the base circle radius does not change, the involutes also do not change. What does change, however, is the part of the involute that is used as the active profile, and the circumferential spacing of the involutes (base pitch remains constant). With positive profile shift, the part of the involute that is used as the active profile is farther out on the involute, which means the average radius of curvature of the profile is larger, reducing contact stresses slightly. Furthermore, the two involutes that form a tooth are spaced farther apart circumferentially, resulting in a thicker, stronger tooth.

Limits for Profile Shift

An upper limit on profile shift results from the fact that as profile shift increases, the tip of the gear tooth becomes narrower. The generally accepted minimum for the normal tooth tip width is 0.3 m_n. A lower limit on profile shift results from the fact that if profile shift decreases enough, the gear tooth will become undercut during the generating process. While it is not unusual to approach the upper limit for profile shift, there is rarely any reason to approach the lower limit. The typical range for profile shift coefficients is:

$$-0.5 \le x \le 1.0 \qquad \text{(Ref. 3, p. 155)} \qquad \text{Eq. 1}$$

In a gearset where the sum of pinion and gear profile shifts is positive, operating center distance and pressure angle will be greater than reference center distance and pressure angle. Operating center distance typically does not exceed reference center distance by more than 4% (Ref. 3, p. 76). If the reference pressure angle is 20°, the operating pressure angle will typically not exceed 30°.

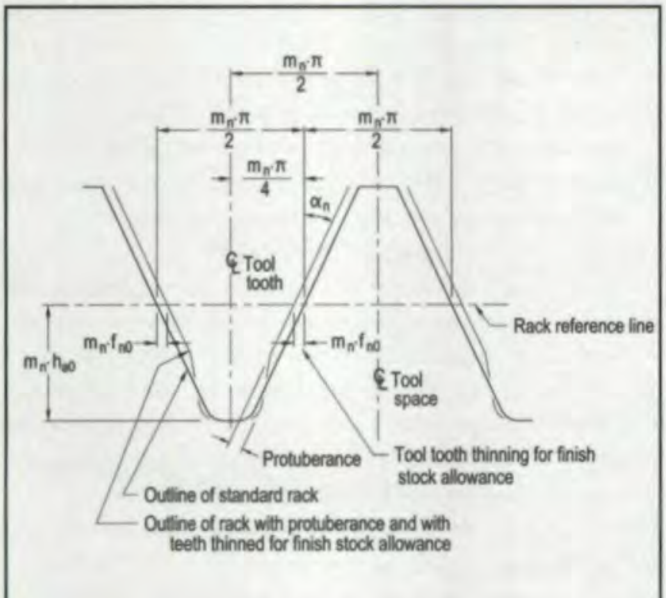

Fig. 1—Terms and symbols related to the tool.

Table 2—Subscripts

(none)	at reference pitch radius
0	tool
1	pinion
2	gear
a	addendum or tip
b	base
f	root
g	generating rack
n	normal
t	transverse
w	at operating pitch radius

For radii, tooth thicknesses, pitches, helix angles and pressure angles: If no subscript is present indicating a particular radius, the parameter applies at the reference pitch radius.

Table 3—Terminology

Terminology used in this article	Other terminology used for the same parameter
Profile shift	Addendum modification Hob offset Cutter offset Correction
Pressure angle	Profile angle
Reference	Standard Generating
Operating	Working
Tip radius	Tip circle radius Outside radius Addendum radius
Base radius	Base circle radius
Tip shortening coefficient	Addendum shortening coefficient
Transverse	Linear
Rack reference line	Rack datum line Rack pitch line
Pitting resistance	Surface durability

Explanations of terms:

1. Reference: This is the term used in Europe for what Americans have historically called "standard." When applied to a gear, it means "at the reference pitch radius" or "at the standard pitch radius." For example, "reference helix angle" means helix angle at the reference (or standard) pitch radius.

2. Reference Line: The reference line of the standard generating rack is the line along which the tooth thicknesses and tooth spaces are both equal to 1/2 of the rack pitch. (The rack normal pitch is equal to $\pi\ m_n$.) The reference line of the manufacturing tool (rack cutter or hob) is the line along which the tool tooth thicknesses and tooth spaces were both equal to 1/2 of the rack pitch before the tool teeth were thinned for finish stock allowance.

3. Profile Shift & Profile Shift Coefficient: Profile shift coefficient is the distance from the reference line of the standard generating rack to the reference pitch circle of a gear in tight mesh with the rack, for a normal module of 1.0. The profile shift coefficient is positive if the reference line of the standard generating rack is farther from the center of the gear than the reference pitch radius, and negative if the reference line of the standard generating rack is closer to the center of the gear than the reference pitch radius. Profile shift, without the term "coefficient," refers to either:

a. The general concept of shifting the standard generating rack reference line off the gear reference pitch circle, or
b. The distance, in units of length, that the standard generating rack reference line is shifted off the gear reference pitch circle, with sign conventions as for profile shift coefficient.

4. Rack Shift & Rack Shift Coefficient: Rack shift coefficient is the distance from the reference line of the manufacturing tool (rack cutter or hob) to the reference pitch circle of the gear being machined, for a normal module of 1.0. The sign conventions are the same as for profile shift coefficient. Rack shift, without the term "coefficient," refers to either:

a. The general concept of shifting the manufacturing tool (rack cutter or hob) reference line off the gear reference pitch circle, or
b. The distance, in units of length, that the manufacturing tool (rack cutter or hob) reference line is shifted off the gear reference pitch circle, with sign conventions as for profile shift coefficient.

The rack shift & rack shift coefficient will typically be slightly different than the profile shift & profile shift coefficient. Tooth thinning considerations will tend to make the rack shift less than the profile shift, and finish stock allowance can tend to make the rack shift more than or less than the profile shift.

5. Normalized: A dimensionless value expressed as a multiple or fraction of normal module. To obtain a normalized value from a non-normalized value, divide the non-normalized value (which will be in millimeters or inches) by the normal module, or multiply it by the diametral pitch.

Figures 2 and 3 illustrate what can happen when excessive profile shift is used.

In Figure 2, positive profile shift eliminated undercut on a pinion that would have been undercut without positive profile shift, but the profile shift was excessive. It resulted in a tooth tip width of 0.111 m_n—much below the recommended minimum of 0.3 m_n. With a larger number of teeth or less positive profile shift, the tip narrowing would not be as severe.

In Figure 3, a pinion is shown that would not be undercut with zero or positive profile shift. A large negative profile shift was used, resulting in severe undercut.

Rack Shift

The concept of rack shift is introduced to accommodate the fact that the manufacturing tool may be at a different location than the theoretical standard generating rack. The gear's performance in terms of pitting resistance and scuffing resistance is based on the location of the theoretical standard generating rack, but for practical manufacturing and operating considerations—as explained below—the manufacturing tool usually must be at a different location than the theoretical standard generating rack.

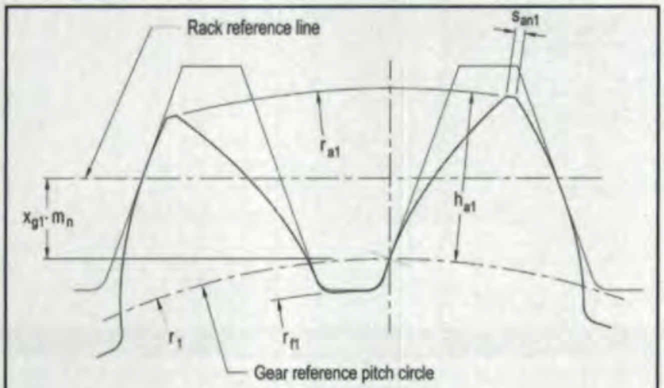

Spur gear
20 degree normal pressure angle
16 teeth
0.9 rack shift coefficient
No tip shortening
1.25 normalized tool addendum
0.20 normalized tool tip radius
Standard rack (tooth space = tooth thickness along rack reference line)

Fig. 2—Excessive profile shift results in narrow tooth tip width.

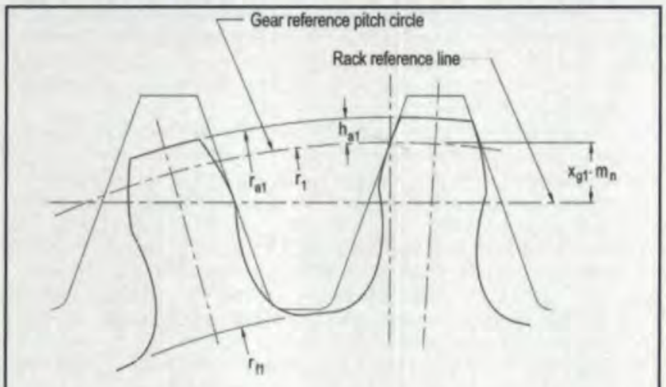

Spur gear
20 degree normal pressure angle
19 teeth
–0.7 rack shift coefficient
No tip shortening
1.25 normalized tool addendum
0.20 normalized tool tip radius
Standard rack (tooth space = tooth thickness along rack reference line)

Fig. 3—Large negative profile shift results in severe undercut.

If a pair of gears were made to exact profile shift with a standard generating rack, and mounted at exact theoretical center distance, there would be no backlash—the gears would be in tight mesh. In practice, finished gear teeth must be slightly thinner than they would be if manufactured to the exact profile shift, to allow backlash, thereby preventing binding and interference. This is accomplished by shifting the generating rack in toward the center of the gear by a predetermined amount. For purposes of pressure angle calculations and pitting resistance, the gear still performs exactly the same as it would if it were at exact profile shift—the involutes and tip radii have not changed; the involutes of any given tooth are just circumferentially closer together. The tooth thinning does, however, weaken the tooth slightly with regard to bending strength; ISO and AGMA ratings take this into account.

If the teeth are to be finished after hobbing by grinding or shaving, extra stock must be left to allow for this finishing. There are three situations that must be considered in this regard:

a. A standard rack is used, so the rack must be shifted away from the center of the gear to leave stock for finishing;
b. A rack with teeth thinned by the exact amount necessary for finish allowance is used, so no change in rack position is necessary for finish allowance; and
c. A rack with thinned teeth is used, but the teeth are not thinned by the exact amount necessary for finish allowance. In this case, the rack will have to be shifted either closer to or farther from the center of the gear to get the correct amount of finish allowance. The rack will need to be moved closer to the center of the gear if the tooth thinning of the rack is greater than the exact amount necessary for finish allowance; the rack will need to be moved farther from the center of the gear if the tooth thinning of the rack is less than the exact amount necessary for finish allowance.

Optimum Profile Shift

If the center distance is not fixed by the application, the designer is free to use negative, zero or positive values for profile shift coefficient for either pinion or gear, and the pinion and gear profile shift coefficients are not required to have any particular mathematical relationship to each other. It is common for pinion profile shift to be positive, to thicken and strengthen the pinion teeth, and for gear profile shift to be negative, to slightly thin the gear teeth, thereby balancing bending strength with the pinion teeth. Another advantage of positive shift in the pinion and negative shift in the gear is that this combination increases recess action for speed reducers, resulting in a smoother-running gearset (Ref. 3, pp. 163, 164). However, recess action becomes approach action if the gear drives the pinion. Therefore, profile shift must be used with caution for speed increasers, which are often designed with profile shift to balance specific sliding. When optimized for pitting resistance, bending strength and scuffing resistance, the sum of pinion and gear profile shifts is nearly always zero or positive. While optimum profile shifts for these criteria are rarely identical, they typically are not far apart, if the pinion has an adequate number of teeth (Ref. 4). Also, while the designer must decide which parameters are to be favored in terms of optimum profile shift, none of them will be far off optimum. This article does not address optimization of profile shift coefficients. For optimization of profile shift coefficients, see Reference 4, Annex A.

Tip Shortening

There are three tooth length options in common use:

1. Full-length teeth (no tip shortening),
2. Standard working depth, and
3. Standard tip-to-root clearance.

Options 1 and 2 sometimes do not give adequate tip-to-root clearance when the operating center distance is significantly greater than the standard center distance, so the algorithm is based on option 3: standard tip-to-root clearance. Standard tip-to-root clearance means that the normalized tip-to-root clearance will be equal to the normalized tool addendum minus 1.00.

Example that Demonstrates the Need for Tip Shortening

When profile shift is used, the sum of the two profile shifts is almost always zero or positive. When the sum of the two profile shifts is positive, the operating center distance is greater than the standard center distance, but not by as much as the sum of the profile shifts. Table 4 shows two different configurations of a 5-diametral-pitch (0.20"-module) spur gear pair: one configuration without profile shift, the other configuration with profile shift.

The equations used to determine the center distance in the last column of Table 4 are not shown in this article, but can be found in Reference 1, page 47 (equations 72–73). The equations require the use of the inverse involute function, which can be found in Reference 2, page 6.6 (equations 6.25–6.29).

In the last column, the tip and root radii of both pinion and gear have grown. The pinion radius has grown by 0.18", and gear radius has grown by 0.14", for a total of 0.18" + 0.14" = 0.32". But the center distance has only increased by 6.78" –

Table 4—Tip Shortening Example

Pinion tooth number	25	
Gear tooth number	40	
Module (inches)	0.20	
Reference pressure angle (degrees)	20	
Generating tool normalized addendum	1.25	
	Gearset without profile shift	**Gearset with profile shift**
Pinion profile shift coefficient	0.00	0.90
Gear profile shift coefficient	0.00	0.70
Pinion root circle radius (inches)	2.2500	2.4300
Gear root circle radius (inches)	3.7500	3.8900
Pinion tip radius, unshortened (inches)	2.7000	2.8800
Gear tip radius, unshortened (inches)	4.2000	4.3400
Operating center distance (inches)	6.5000	6.7800
Pinion tip (unshortened) to gear root circle clearance (inches)	0.0500	0.0100
Gear tip (unshortened) to pinion root circle clearance (inches)	0.0500	0.0100

6.50" = 0.28", so the tip-to-root clearances have been reduced by 0.32" – 0.28" = 0.04". The new clearances are only 0.01" for a 5-DP gearset! These are dangerously low tip-to-root clearances, and they indicate a high probability of tip-to-fillet interference.

With certain combinations of parameters, *the tips of unshortened gear teeth can actually theoretically lie below the root circle of the mating gear*. This is why tip shortening is necessary when profile shift is used. The algorithm below includes equations for tip shortening. The results of tip shortening are given in terms of shortened addenda and tip radii.

Subtleties come up when considering tip shortening in gears with finish stock allowance left on. In Europe, it is standard practice to use a tool (rack cutter or hob) that has teeth thinned by the exact amount needed to leave the desired amount of stock for finishing. This means that the tool does not have to be shifted at all for finish stock allowance. However, the rack still gets shifted inward for gear tooth thinning. This inward shift results in a reduced root radius. The tip shortening equations (Eqs. 26–28) use the profile shift coefficients rather than the rack shift coefficients. The reduction of root radius means the clearance obtained is slightly greater than assumed by the tip shortening equations. This difference will be seen in the results of the clearance equations (Eqs. 31–32), which will be greater than h_{a0} minus 1.00, if the rack shift is less than the profile shift. This increase in clearance is not seen as a problem.

A problem does arise, though, when the generating rack teeth have been thinned by less than the amount required for finish stock allowance. In this case, the generating rack has to be shifted inward for tooth thinning and outward for finish stock allowance. If the outward shift for finish stock allowance is greater than the inward shift for tooth thinning, the root radius will be larger than assumed by the tip shortening equations, and reduced tip-to-root clearances will result. One solution to this problem is to use the rack shift coefficients rather than the profile shift coefficients in the tip shortening equations (Eqs. 26–28). This solution has the unfortunate result that tip shortening becomes a function of finish stock allowance and backlash, *but it does give correct results for tip shortening and tip-to-root* clearance. Regardless of whether the rack shift coefficients or the profile shift coefficients are used in the tip shortening equations, the results of the root radius equations (Eqs. 24–25) and the clearance equations (Eqs. 31–32) will be correct, because they use the rack shift coefficients.

There is a price to be paid for tip shortening, because it results in smaller gear tip radii and reduced contact ratio, but this takes back only a small portion of what is gained by using profile shift.

Algorithm

If the algorithm does not yield a satisfactory gear profile shift coefficient, x_2, and it is acceptable to change the helix angle, changing the helix angle will change the pinion and gear reference and base radii, thereby also changing the gear profile shift coefficient. The helix angle can be changed iteratively until a satisfactory gear profile shift coefficient is obtained. There is another procedure, not addressed in this article, which yields operating center distance when profile shift coefficients are already established for both pinion and gear. The procedure can be found in Reference 1, pages 46–47.

The algorithm gives tooth thicknesses after final finish operations. Rack shift equations give rack shift coefficients for cutting teeth with extra material left for finish allowance, but equations for tooth thicknesses before finishing are not given. If stock allowance for finishing is not required, f_{n1} and f_{n2} should be set to zero. If the rack teeth have not been thinned for stock allowance for finishing, f_{n01} and f_{n02} should be set to zero.

The algorithm calculates the following:

- Radii: reference, operating, base, root and tip;
- Reference center distance;
- Tooth thicknesses: reference, operating and tip;
- Generating rack shift coefficients;
- Pressure angles: transverse reference, normal operating, transverse operating and tip;
- Helix angles: base, operating and tip;
- Base pitches: normal and transverse;
- Sum of profile shift coefficients;
- Gear profile shift coefficient, x_2;
- Tip shortening coefficient;
- Addenda;
- Tip-to-root clearances; and
- Tooth thinning for backlash.

The user must provide the following parameters:

m_n	Normal module.
z_1 , z_2	Number of teeth for pinion and gear.
β	Reference helix angle.
α_n	Normal pressure angle.
x_1	Pinion profile shift coefficient.
a	Operating center distance.
j_{n1}	Backlash in the normal plane due to pinion tooth thinning, normalized.
j_{n2}	Backlash in the normal plane due to gear tooth thinning, normalized.
f_{n1}, f_{n2}	Total stock allowance per side for finishing, in the normal plane, normalized.
f_{n01}, f_{n02}	Stock allowance per side for finishing, in the normal plane, built into the tool, normalized.
h_{a01}, h_{a02}	Tool addenda, normalized.

It is assumed the addendum of a standard gear tooth without profile shift before tip shortening is 1.00 m_n.

Units are defined in Table 1. Note that many parameters are dimensionless because they are normalized (expressed as a fraction or multiple of normal module).

For those who are more familiar with diametral pitch, the algorithm still can be used by first converting normal diametral pitch to normal module with the following equation:

$$\text{Normal Module} = \frac{1}{\text{Normal Diametral Pitch}} \qquad \text{Eq. 2}$$

For example, 4 Normal Diametral Pitch = 0.25" Normal Module.

The involute function is used several times in the algorithm. The involute function is defined as follows:

$$\text{inv}\,\alpha = \tan\alpha - \alpha \qquad \text{Eq. 3}$$

where the angle α is in radians.

The algorithm applies to external parallel-axis spur and helical gearsets only. For purposes of this algorithm, spur gears are considered helical gears with 0° helix angle.

Gear ratio:

$$u = \frac{z_2}{z_1} \qquad \text{Eq. 4}$$

Pinion reference pitch radius:

$$r_1 = \frac{z_1 \cdot m_n}{2 \cdot \cos\beta} \qquad \text{Eq. 5}$$

Gear reference pitch radius:

$$r_2 = r_1 \cdot u \qquad \text{Eq. 6}$$

Pinion operating pitch radius:

$$r_{w1} = \frac{a}{u+1} \qquad \text{Eq. 7}$$

Gear operating pitch radius:

$$r_{w2} = a - r_{w1} \qquad \text{Eq. 8}$$

Transverse reference pressure angle:

$$\alpha_t = \arctan\left(\frac{\tan\alpha_n}{\cos\beta}\right) \qquad \text{Eq. 9}$$

Pinion base radius:

$$r_{b1} = r_1 \cdot \cos\alpha_t \qquad \text{Eq. 10}$$

Gear base radius:

$$r_{b2} = r_{b1} \cdot u \qquad \text{Eq. 11}$$

Normal base pitch:

$$p_N = m_n \cdot \pi \cdot \cos\alpha_n \qquad \text{Eq. 12}$$

Transverse base pitch:

$$p_b = \frac{2 \cdot \pi \cdot r_{b1}}{z_1} \qquad \text{Eq. 13}$$

Base helix angle:

$$\beta_b = \arccos\left(\frac{p_N}{p_b}\right) \qquad \text{Eq. 14}$$

Transverse operating pressure angle:

$$\alpha_{wt} = \arccos\left(\frac{r_{b1} + r_{b2}}{a}\right) \qquad \text{Eq. 15}$$

Normal operating pressure angle:

$$\alpha_{wn} = \arcsin(\cos\beta_b \cdot \sin\alpha_{wt}) \qquad \text{Eq. 16}$$

Sum of profile shift coefficients:

$$\sum x = \frac{z_1 + z_2}{2} \cdot \frac{\text{inv}\,\alpha_{wt} - \text{inv}\,\alpha_t}{\tan\alpha_n} \qquad \text{Eq. 17}$$

Gear profile shift coefficient:

$$x_2 = \sum x - x_1 \qquad \text{Eq. 18}$$

Reference center distance:

$$a_d = r_1 + r_2 \qquad \text{Eq. 19}$$

Pinion tooth thinning for backlash:

$$\Delta s_{n1} = j_{n1} \cdot \frac{a_d}{a} \qquad \text{Eq. 20}$$

Gear tooth thinning for backlash:

$$\Delta s_{n2} = j_{n2} \cdot \frac{a_d}{a} \qquad \text{Eq. 21}$$

Pinion rack shift coefficient:

$$x_{g1} = x_1 - \frac{\Delta s_{n1}}{2 \cdot \tan \alpha_n} + \frac{f_{n1} - f_{n01}}{\tan \alpha_n} \qquad \text{Eq. 22}$$

Gear rack shift coefficient:

$$x_{g2} = x_2 - \frac{\Delta s_{n2}}{2 \cdot \tan \alpha_n} + \frac{f_{n2} - f_{n02}}{\tan \alpha_n} \qquad \text{Eq. 23}$$

Pinion root radius:

$$r_{f1} = r_1 - m_n \cdot (h_{a01} - x_{g1}) \qquad \text{Eq. 24}$$

Gear root radius:

$$r_{f2} = r_2 - m_n \cdot (h_{a02} - x_{g2}) \qquad \text{Eq. 25}$$

Tip shortening coefficient:

$$k = \sum x - \frac{a - a_d}{m_n} \qquad \text{Eq. 26}$$

Shortened pinion addendum:

$$h_{a1} = m_n \cdot (1 + x_1 - k) \qquad \text{Eq. 27}$$

Shortened gear addendum:

$$h_{a2} = m_n \cdot (1 + x_2 - k) \qquad \text{Eq. 28}$$

Pinion tip radius:

$$r_{a1} = r_1 + h_{a1} \qquad \text{Eq. 29}$$

Gear tip radius:

$$r_{a2} = r_2 + h_{a2} \qquad \text{Eq. 30}$$

Pinion tip to gear root circle clearance:

$$c_{12} = a - r_{a1} - r_{f2} \qquad \text{Eq. 31}$$

Gear tip to pinion root circle clearance:

$$c_{21} = a - r_{a2} - r_{f1} \qquad \text{Eq. 32}$$

Pinion normal circular tooth thickness at reference pitch radius:

$$s_{n1} = m_n \cdot \left(\frac{\pi}{2} + 2 \cdot x_1 \cdot \tan \alpha_n - \Delta s_{n1} \right) \qquad \text{Eq. 33}$$

Gear normal circular tooth thickness at reference pitch radius:

$$s_{n2} = m_n \cdot \left(\frac{\pi}{2} + 2 \cdot x_2 \cdot \tan \alpha_n - \Delta s_{n2} \right) \qquad \text{Eq. 34}$$

Pinion transverse circular tooth thickness at reference pitch radius:

$$s_{t1} = \frac{s_{n1}}{\cos \beta} \qquad \text{Eq. 35}$$

Gear transverse circular tooth thickness at reference pitch radius:

$$s_{t2} = \frac{s_{n2}}{\cos \beta} \qquad \text{Eq. 36}$$

Transverse pressure angle at pinion tooth tip:

$$\alpha_{at1} = \arccos \left(\frac{r_{b1}}{r_{a1}} \right) \qquad \text{Eq. 37}$$

Transverse pressure angle at gear tooth tip:

$$\alpha_{at2} = \arccos \left(\frac{r_{b2}}{r_{a2}} \right) \qquad \text{Eq. 38}$$

Pinion transverse tooth tip width:

$$s_{at1} = r_{a1} \cdot \left(\frac{s_{t1}}{r_1} + 2 \cdot (\text{inv}\, \alpha_t - \text{inv}\, \alpha_{at1}) \right) \qquad \text{Eq. 39}$$

Gear transverse tooth tip width:

$$s_{at2} = r_{a2} \cdot \left(\frac{s_{t2}}{r_2} + 2 \cdot (\text{inv}\, \alpha_t - \text{inv}\, \alpha_{at2}) \right) \qquad \text{Eq. 40}$$

Pinion helix angle at tip radius:

$$\beta_{a1} = \arctan \left(\frac{\tan \beta_b}{\cos \alpha_{at1}} \right) \qquad \text{Eq. 41}$$

Gear helix angle at tip radius:

$$\beta_{a2} = \arctan \left(\frac{\tan \beta_b}{\cos \alpha_{at2}} \right) \qquad \text{Eq. 42}$$

Pinion normal tooth tip width:

$$s_{an1} = s_{at1} \cdot \cos \beta_{a1} \qquad \text{Eq. 43}$$

Gear normal tooth tip width:

$$s_{an2} = s_{at2} \cdot \cos \beta_{a2} \qquad \text{Eq. 44}$$

Pinion transverse circular tooth thickness at operating pitch radius:

$$s_{wt1} = r_{w1} \cdot \left(\frac{s_{t1}}{r_1} + 2 \cdot (\text{inv}\, \alpha_t - \text{inv}\, \alpha_{wt}) \right) \qquad \text{Eq. 45}$$

Gear transverse circular tooth thickness at operating pitch radius:

$$s_{wt2} = r_{w2} \cdot \left(\frac{s_{t2}}{r_2} + 2 \cdot (\text{inv}\, \alpha_t - \text{inv}\, \alpha_{wt}) \right) \qquad \text{Eq. 46}$$

Operating helix angle:

$$\beta_w = \arctan \left(\frac{\tan \beta_b}{\cos \alpha_{wt}} \right) \qquad \text{Eq. 47}$$

Pinion normal circular tooth thickness at operating pitch radius:

$$s_{wn1} = s_{wt1} \cdot \cos \beta_w \qquad \text{Eq. 48}$$

Gear normal circular tooth thickness at operating pitch radius:

$$s_{wn2} = s_{wt2} \cdot \cos \beta_w \qquad \text{Eq. 49}$$

Acknowledgments

The author thanks *Gear Technology* technical editor Robert Errichello for suggesting the topic for this article, and for his editing services.

References

1. Maag Gear Co. *Maag Gear Book*, Maag Gear Co., Zurich, 1990.
2. Errichello, Robert. *Dudley's Gear Handbook*, Chapter 6, McGraw-Hill, New York, 1991.
3. Colbourne, J.R. *The Geometry of Involute Gears*, Springer-Verlag, New York, 1987.
4. AGMA 901-A92, "A Rational Procedure for the Preliminary Design of Minimum Volume Gears," AGMA, Alexandria, Virginia, 1992.
5. AGMA 908-B89, "Geometry Factors for Determining the Pitting Resistance and Bending Strength of Spur, Helical, and Herringbone Gear Teeth," AGMA, Alexandria, Virginia, April 1989.
6. AGMA 2001-C95, "Fundamental Rating Factors and Calculations for Involute Spur and Helical Gear Teeth," AGMA, Alexandria, Virginia, January 1995.

Phillips D. Rockwell, P.E. *owns Bay Machine Design, a San Francisco Bay area consulting mechanical engineering firm, specializing in the design of industrial machinery and automation systems. He has designed steel mill machinery, packaging machinery, positioners and optical inspection equipment. He is a registered mechanical engineer in California, a technical consultant member of AGMA, and a member of ASME, SME, ASM, NSPE and STLE. He can be reached by e-mail at pdr@baymachinedesign.com.*

Tell Us What You Think . . .
For more information about Bay Machine Design, **circle 311.**

If you found this article of interest and/or useful, please **circle 309.**
If you did not care for this article, ***circle 310.***

If you would like to respond to this or any other article in this edition of *Gear Technology*, please fax your response to the attention of Randy Stott, managing editor, at 847-437-6618 or send e-mail messages to *people@geartechnology.com.*

Gleason, Mahr Team Up On Gear-Metrology Products

Gleason Corp. and Mahr GmbH allied with each other to develop, promote, sell and service gear-metrology products around the world, according to a press release.

Effective Jan. 1, 2002, Gleason will be responsible worldwide for selling and supporting Mahr's gear-metrology products, including Mahr's double-flank roll testers and its gear-specific version of its PRIMAR inspection system.

Also, the two companies will work together to develop new products to expand the current line of gear-metrology products. The products sold under the alliance will have the brand name "Gleason Mahr."

David J. Burns, Gleason's president and COO, said he was confident that combining Gleason's capabilities in gear processing solutions with Mahr's in metrology would result in "an impressive range of gear-metrology products and services."

Thomas Keidel, Mahr's managing director and chairman of its board of directors, said Mahr was in a manufacturing environment where it's increasingly important to combine metrology with the manufacturing process to economically develop and produce superior products.

Keidel added Mahr was confident that its partnership with Gleason would allow Mahr "to bring our metrology know-how even closer to where it is required."

Inductoheat Hires New Director of Gear-Hardening Development


Madhu Chatterjee

Inductoheat Inc. hired Madhu Chatterjee as director of gear-hardening development and special projects.

According to a press release, Chatterjee will be responsible for aiding research and development on gear-hardening projects, as well as working to develop new technology in several different projects.

Chatterjee previously worked for General Motors Corp./Delphi Automotive for 24 years. He holds four patents and several awards. Also, he has three patents pending.

Hawk Corp. Hires New President for its Powder-Metal Group

Hawk Corp. of Cleveland, OH, hired Michael Corkran as president of its powder-metal group, according to a press release. The group supplies powder-metal parts for industrial applications, including gears and other motor, pump and transmission elements.

As president, Corkran will create a new headquarters in Solon, OH, at Hawk's recently acquired metal-injection-molding facility.

Jeff Berlin, Hawk's president and COO, said Corkran has "an extremely strong operating background, with particular success in manufacturing engineered products and growth through international expansion."

Corkran previously worked for Reltec Corp., a manufacturer of telecommunication equipment, as president of its North American and Asian regions. Also, he started his career at Reliance Electric, where he held a number of management positions.

Berlin added that Corkran's background fits "perfectly with our strategic plan for the powder-metal business, where we will emphasize new product development and growth overseas."

American Axle Gets Gear Forging Agreement with Ford

American Axle & Manufacturing Holdings Inc. (AAM) will provide Ford Motor Co. with net-shape differential gears for automatic transmissions in selected front-wheel-drive Ford vehicles, according to an AAM press release.

The gears will be forged at AAM's Tonawanda Forge in New York using the facility's flashless net-shape pinion and side gear technology, then will be final machine finished at the company's nearby Cheektowaga facility.

According to AAM, the net-formed gear teeth provide increased strength, which allows drivelines to transmit increased torque while using the same size gears.

"We originally developed net-shape gears for our own quiet PowerDense axles," says Allan R. Monich, vice president of manufacturing, forging division. "We have now transferred that technology to transmission differential applications and are able to offer that technological advantage to our customers." ○

Tell Us What You Think . . .
If you found this column of interest and/or useful, please **circle 307.**

If you did not care for this column, **circle 308.**

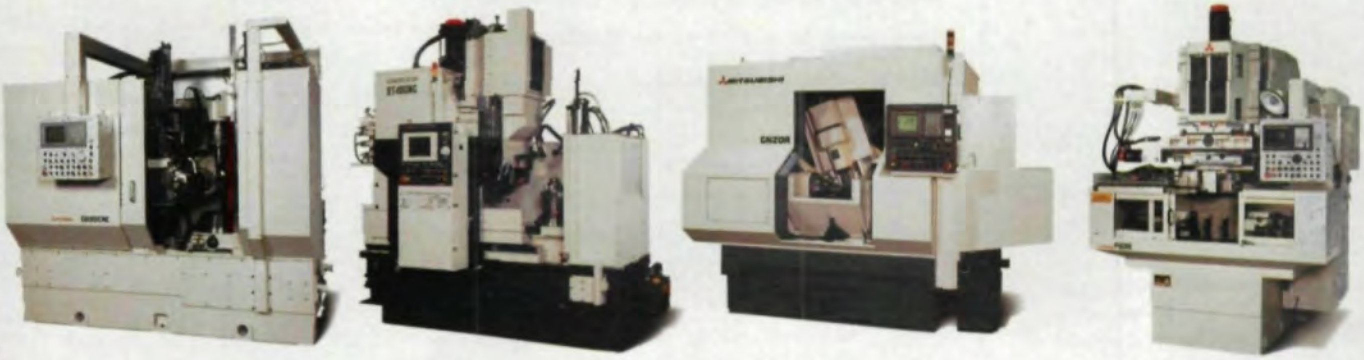

Systematic Investigations on the Influence of Viscosity Index Improvers on EHL Film Thickness

Bernd-Robert Höhn, Klaus Michaelis and Franz Kopatsch

Nomenclature

A	deformed area of disk capacitor
C	capacitance of disk capacitor
C	thermal correction factor acc. Murch/Wilson (Ref. 12)
E_1, E_2	Young's modulus of contact bodies
E'	reduced Young's modulus
F_N	normal force
G	EHL-parameter of elasticity
L	thermal load factor acc. Murch/Wilson (Ref. 12)
M_w	weight average molecular weight
P	polymer correction factor
R	reduced radius of curvature
SSI	shear stability index
U	EHL parameter of velocity
VI	viscosity index
W	EHL parameter of load
b	deformed Hertzian contact width
d_a	tip circle
d_b	base circle
d_w	pitch circle
f	frequency of resonance circuit
h_{meas}	measured lubricant film thickness
h_{min}	minimum film thickness calculated acc. Dowson/Higginson (Ref. 5)
h_0	film thickness in the parallel gap calculated acc. Ertel/Grubin (Refs. 6 and 8)
l_{eff}	disk width
p_H	Hertzian contact pressure
r_1, r_2	radius of curvature of contact bodies
s	slip ratio ($s = 1 - v_2/v_1$)
v_1, v_2	surface velocity of contact bodies ($v_2 < v_1$)
v_Σ	hydrodynamic velocity ($v_\Sigma = v_1 + v_2$)
α	pressure-viscosity coefficient
α_t	temperature coefficient of dynamic viscosity
γ	shear rate
ε_{oil}	relative dielectric coefficient of the oil
ε_0	electric field constant ($\varepsilon_0 = 8.8542 \cdot 10^{-12}$ $C/(Vm)$)
η	dynamic viscosity
η_M	dynamic viscosity at bulk temperature
ϑ	temperature
ϑ_M	average bulk temperature ($\vartheta_M = (\vartheta_1 + \vartheta_2)/2$)
ϑ_1, ϑ_2	bulk temperature of contact bodies
ϑ_{oil}	oil inlet temperature
λ	heat conductivity of lubricant (mineral oil: $\lambda \approx 0.133$ $W/(m \cdot K)$)
ν	kinematic viscosity
ν_1, ν_2	Poisson's ratio of contact bodies
ω	angle velocity

Introduction

Mineral-oil-base lubricants show a significant decrease of kinematic viscosity with rising temperature, as exemplified in Figure 1 by lubricants for vehicle gears. An important attribute of lubricants is their viscosity index (VI), according to DIN/ISO 2909 (Ref. 4). Viscosity index is a calculated coefficient, which characterizes the change of viscosity of lubricants as a function of temperature. A high viscosity index represents a low variation of viscosity due to temperature and vice versa. A low viscosity-temperature-dependence is required for lubricants that are operated at significantly varying temperature conditions, such as vehicle engine and gear lubricants in summer and winter time. This way, the oils remain flowing and pumpable at low temperatures on the one hand; and on the other hand, sufficiently thick lubricant films can be formed at higher temperatures for a safe separation of the surfaces.

A deliberate improvement of the viscosity temperature behavior can be achieved by blending an oil with polymer additives as viscosity-index improvers, such as polyalkylmethacrylate (PMA), olefin copolymer (OCP), styrene butadiene copolymer (SBC) or polyisobutylene (PIB). This way, polymer-free monograde oils can be converted into multigrade oils, which are used in large quantities as engine oils in vehicles (e.g. SAE 15W-40), as gear oils in manual transmissions in vehicles (e.g. SAE 75W-90, see Fig. 1) or in automatic transmissions (e.g. ATF DEXRON® type oils). Universal oils for tractors and earth-movers (e.g. UTTO), which can be used for hydraulics and gears, are multigrade oils as well.

The viscosity-increasing effect of polymer additives at laboratory conditions is known and can be proved. However, their efficiency at EHL conditions of high pressure, high shear rate and high temperature, such as in gear or roller-bearing contacts, is questionable. Polymer-containing oils can suffer from a temporary viscosity loss by high shear rates in an EHL contact, and they can suffer from a permanent viscosity loss by a partial mechanical destruction of the polymers during operation. That results in a lower operating viscosity and, hence, worse lubricating conditions than one would expect according to the viscosity data determined at laboratory conditions with the fresh oil.

The lubricant film thickness significantly influences the micropitting and wear performance of gear applications and, to a smaller extent, it also affects the pitting and scuffing performance. Knowledge of the actual lubricant film thickness in a gear contact is therefore essential for a reliable estimation of the failure risks of wear and micropitting, which are recently more and more the focus of interest.

For that reason, the efficiency of viscosity index (VI) improvers in EHL contacts was investigated by systematic measurements of the lubricant film thickness. Various types of polymers with various molecular weights and concentrations in the base oil were included in the test program in order to determine the influence of each parameter on the formation of lubricant films separately from each other.

Test Lubricants

The investigations were carried out with more than 20 test lubricants, which were blended especially for this research project. The base oils were two straight-paraffin-base mineral oils, M32 and M100, of the viscosity grades ISO VG 32 and ISO VG 100. The polymers that were used consisted of PMA (polyalkylmethacrylate), PIB (polyisobutylene), OCP (olefin copolymer), SBC (styrene butadiene copolymer) and STAR (star-shaped styrene isoprene copolymer). For each type of those polymers, a set of five different blends was investigated, which is shown in Table 1 for the polymer PMA, as an example. Each polymer type was available with low molecular weight (designated by the codes PMA1, OCP1, etc.) and high molecular weight (PMA2, OCP2, etc.). The polymers with low molecular weight were added in low concentration (PMA1L, OCP1L, etc.) and high concentration (PMA1H, OCP1H, etc.) to the base oil M100 and in very high concentration to the base oil M32 (PMA1VH, OCP1VH, etc.). The polymers with high molecular weight were added in low concentration to base oil M100 (PMA2L, OCP2L, etc.) and in high concentration to base oil M32 (PMA2H, OCP2H, etc.).

The polymer concentration in each blend was chosen with respect to equal kinematic viscosities v_{100} of all test lubricants at 100°C, so that the lubricant film thicknesses of all oils could be directly compared at high temperature. Emphasis was put on higher-viscous blends (v_{100} = 20 mm²/s), in order to get measurable film thicknesses at high temperatures up to 110°C, at which the investigations were performed. For a direct comparison with a straight mineral oil, a straight-paraffin-base mineral oil M240 with the same kinematic viscosity of v_{100} = 20 mm²/s at 100°C was included in the set of test lubricants.

Table 1–Systematics of test lubricants for PMA-containing oils as examples.

Code of test oil	Molecular weight		Concentration			Base oil		Viscosity v_{100} in mm²/s	
	low	high	low	high	very high	M32	M100	12.6	20
PMA1L	X		X				X	X	
PMA1H	X			X			X		X
PMA2L		X	X				X		X
PMA2H		X		X		X			X
PMA1VH	X				X	X			X

The investigation of a set of five different blends, as shown in Table 1 for each type of polymers, gives information about:

• the influence of the concentration of polymers with the same molecular weight in the same base oil (PMA1L and PMA1H),

• the influence of the molecular weight of the polymers in blends with the same viscosity at 100°C and with the same base oil, and

• the influence of the base oil viscosity in blends with the same polymer type (low and high molecular weight) and with the same viscosity at 100°C.

The STAR-type polymers were investigated in two blends only, which were equivalent to the blends with high molecular weight (…2L, …2H).

Shear Stability of Investigated Polymers

Permanent Viscosity Loss. Polymer-containing oils can suffer a permanent viscosity loss when being subject to mechanical loads, which can shred the polymer chains. That process is not reversible.

All polymer-containing test oils were subjected to a 20-hour tapered-roller-bearing shear test (KRL-shear test) according to CEC L-45-A-99 (Ref. 2), in order to determine the permanent viscosity loss by shearing. In this test, a tapered roller bearing 32008XQ is lubricated

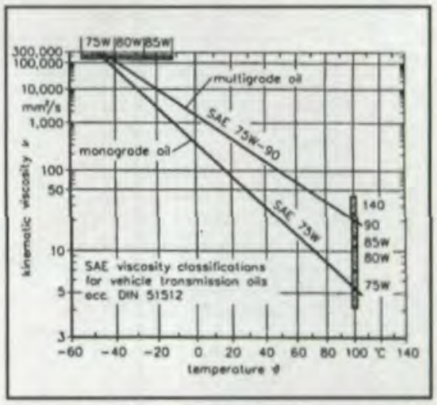

Figure 1—Difference between monograde and multigrade gear oils for vehicles.

Professor Dr.-Ing. Bernd-Robert Höhn
is head of the Institute of Machine Elements and the Gear Research Centre, both at the Technical University of Munich, Germany. The centre performs basic and applied research in the fields of load-carrying capacity and tribology of gears and automotive components.

Professor Dr.-Ing. Klaus Michaelis
is research group manager at the Gear Research Centre. He is responsible for experimental elastohydrodynamics and tribology and their application to gear scuffing and wear phenomena.

Dr.-Ing. Franz Kopatsch
is head of the calculation group at Steinbock GmbH, a German manufacturer of electric forklift trucks. A mechanical engineer, he worked from 1994 to 2000 as a scientific assistant at the Gear Research Centre. As an assistant, he performed two research projects on the influence of viscosity-index improvers on EHL-film thickness.

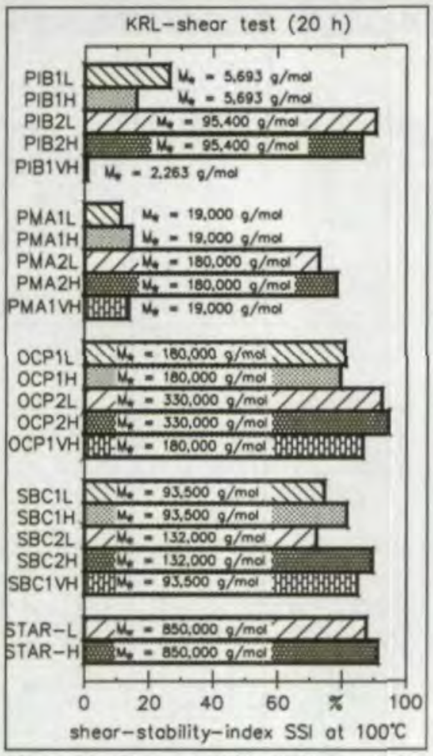

Figure 2—Shear stability indices of the test oils after a KRL-shear test.

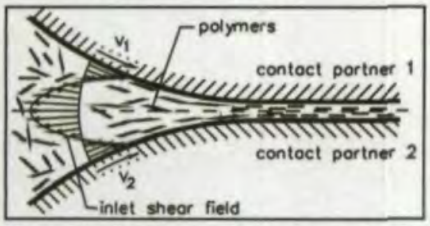

Figure 3—Arrangement of polymers in the inlet shear field of an EHL contact.

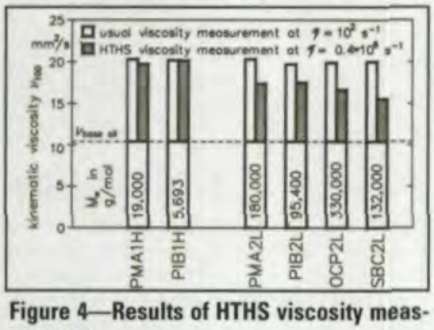

Figure 4—Results of HTHS viscosity measurements.

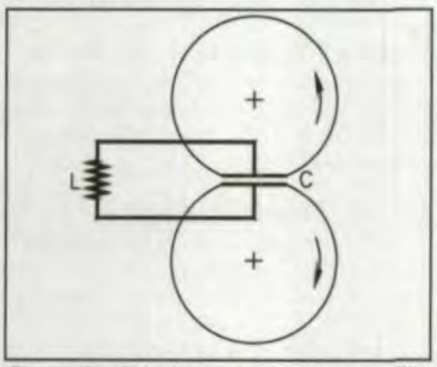

Figure 5—Principle of capacitance film thickness test method.

with 40 ml of the test fluid by dip lubrication at 60°C. The bearing is run for 20 hours at 1,450 rpm and at a load of 5 kN. The kinematic viscosity v_{100} of the test oil is measured before and after the test at 100°C. With this information and the viscosity of the base oil $v_{100,base\ oil}$, the shear stability index (*SSI*) of the polymer in the blend can be calculated. It is defined as:

$$SSI = \frac{(v_{100,fresh} - v_{100,KRL})}{(v_{100,fresh} - v_{100,base\ oil})} \qquad (1)$$

with

$v_{100,fresh}$ = kinematic viscosity in mm²/s of the fresh polymer-containing oil, determined at a temperature of 100°C by using a capillary viscometer,

$v_{100,KRL}$ = kinematic viscosity in mm²/s of the polymer-containing oil after a KRL-shear test according to CEC L-45-A-99 (Ref. 2), determined at a temperature of 100°C by using a capillary viscometer, and

$v_{100,base\ oil}$ = kinematic viscosity in mm²/s of the base oil, determined at a temperature of 100°C by using a capillary viscometer.

The shear-stability index is an indicator for the shear-stability of the polymers. *SSI* = 0% means that the polymer-containing oil has the same viscosity after the KRL-shear test as before, so the polymers are shear-stable. SSI = 100% means that the polymer-containing oil has only the viscosity of the base oil after the KRL-shear test, so the viscosity-increasing effect of the polymers has completely disappeared after the test. In this case, the polymers are unstable against shear.

The shear-stability indices of the polymer-containing oils, which were derived from the KRL-shear tests, are shown in Figure 2. The shear-stability strongly depends on the average molecular weight of the polymers. For example, the test oils containing the polymers PIB1 and PMA1, which have a molecular weight M_w of less than 20,000 g/mole each, show the lowest shear-stability indices after the KRL-shear test, so those polymers are relatively stable against permanent shearing. All of the other polymers that were investigated have molecular weights M_w of more than 90,000 g/mole at fresh-oil condition. The shear-stability indices of the corresponding oils are all more than 70%. That means that after the KRL-shear test, the polymer chains are broken into pieces and hardly able to significantly increase the blend viscosity above the base oil viscosity.

Temporary Viscosity Loss

Long-stretched polymer chains tend to arrange themselves in parallel within a shear field, as shown in Figure 3. That way, the probability of the polymers becoming tangled with each other is reduced and so is the thickening effect of the polymers. This process is reversible. Such a shear field exists in the inlet region of any oil-lubricated EHL contact. It is caused by the back-flow of the surplus oil.

To get information about the temporary viscosity loss, high-temperature-high-shear (HTHS) viscosity measurements were carried out with some of the test oils. A capillary viscometer aided by air pressure was used to increase the velocity of the oils flowing through the capillary. That way, the shear ratio of the oil in the capillary could be increased from $\gamma \approx 10^2\ s^{-1}$ at pure-gravity-induced flow to some $0.4 \cdot 10^6\ s^{-1}$ at air-pressure-aided flow.

The results of the HTHS viscosity measurements are shown in Figure 4 for the oils PMA1H, PIB1H, PMA2L, PIB2L, OCP2L and SBC2L. The temporary viscosity loss of the oils containing long-chain polymers is significantly higher than that of the oils containing short-chain ones. The SBC polymers appear to be especially susceptible to temporary viscosity loss, as they lose about half of their thickening power at the high shear ratio in Figure 4.

Results of Film Thickness Measurements

Test Principle. The measurements were carried out in a twin-disk test rig. The core of the test rig consists of two cylindrical steel disks, each one 80 mm in diameter. They can be driven separately from each other with continuously variable speeds and can be loaded with a normal force F_N. The test oil is injected between both disks. The bulk temperatures ϑ_1 and ϑ_2 of both disks are measured with temperature sensors in boreholes 2 mm below the running surfaces. A detailed description of the test rig and of the test disks is given in Reference 9.

When loaded and thus elastically deformed, both disks and the lubricant between them form a capacitor (see Fig. 5), the capacitance C of which depends on the lubricant film thickness h_{meas}, the relative dielectric coefficient ε_{oil} of the lubricant, the deformed Hertzian contact width b and the disk width l_{eff} according to Equation 2.

$$C = \varepsilon_0 \cdot \varepsilon_{oil} \cdot (A/h_{meas})$$
$$\text{with } A = 2 \cdot b \cdot l_{eff} \qquad (2)$$

The "disk capacitor" is integrated into a resonance circuit, the frequency f of which depends on the capacitance C and a known inductivity L. By using a capacitance-frequency-calibration curve, the capacitance C can be derived from the resonance circuit's frequency f, which is determined by using a frequency counter.

The relative dielectric coefficient of the oil ε_{oil} is measured in a high pressure cell as a function of pressure and temperature. The deformed Hertzian contact width b can be calculated with the Hertzian equations. With that data, the lubricant film thickness h_{meas} of the oil can be calculated from the capacitance C of the disk capacitor by numerical integration. The calculation method used is based on Equation 2. It divides the contact zone into five separate sections with different portions of the entire capacitance and also takes into account the influence of an insulating layer made from Al_2O_3, which is applied to one of the disk surfaces by ion beam sputtering in order to prevent electric shortcuts between the disks. More detailed information about the measuring technique used is given in Reference 13.

Film Thickness of Polymer-Containing Oils. In the following, the most important results of the film thickness measurements of the test oil blends ...1H and ...2L (see Table 1) are presented. A detailed description and discussion of all test results gained in this project can be found in Reference 9.

The viscosity-temperature curves of the blends ...1H and ...2L are shown in Figures 6 and 7. All polymer-containing test oils were blended with equal kinematic viscosities at 100°C of $\nu_{100} = 20$ mm²/s, which is the value of the reference mineral oil M240. The base oil M100 has a kinematic viscosity at 100°C of approximately 10 mm²/s.

Figure 8 shows the measured film thicknesses of the test oils with polymers having low molecular weight and high concentration (PIB1H, OCP1H, SBC1H, PMA1H) and of the straight mineral oils M100 and M240 plotted against the bulk temperature ϑ_M of the disks. $\vartheta_M = (\vartheta_1 + \vartheta_2)/2$ is the average measured bulk temperature of both disks. At high temperatures, the oils PIB1H and PMA1H form film thicknesses similar to the mineral oil M240, which has the same kinematic vis-

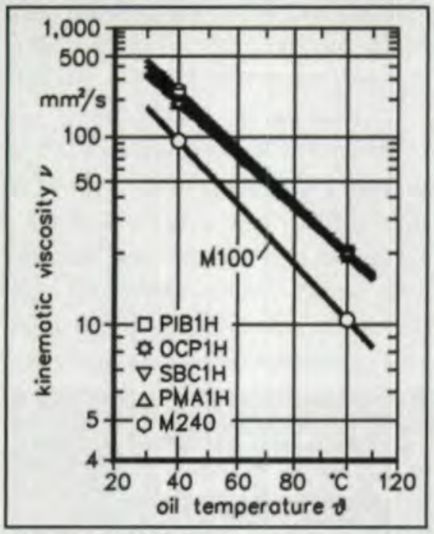

Figure 6—Viscosity temperature curves of test oils ...1H.

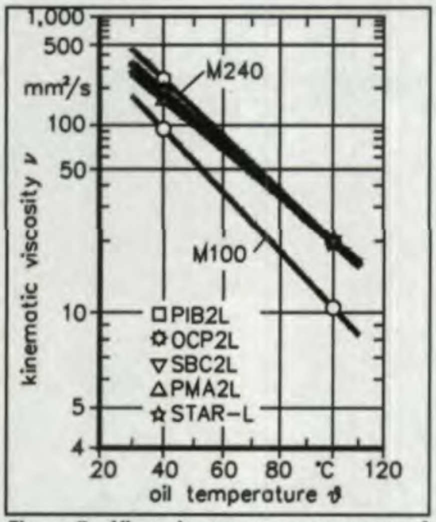

Figure 7—Viscosity temperature curves of test oils ... 2L.

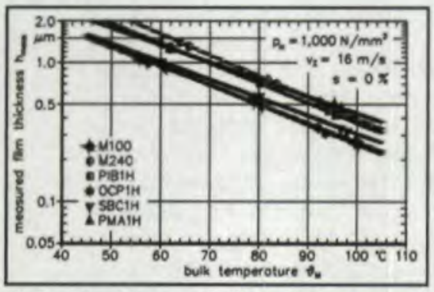

Figure 8—Measured film thicknesses of test oils ... 1H.

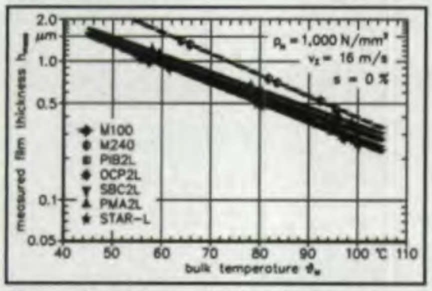

Figure 9—Measured film thicknesses of test oils ... 2L.

cosity v_{100} as the polymer-containing oils. At low temperatures, however, the film thicknesses of PIB1H and PMA1H are lower than those of M240. The VI-improving effect of the polymers PIB1 and PMA1 can be seen quite clearly here.

On the other hand, the oils OCP1H and SBC1H show only very little increase of the film thickness compared to the base oil M100. Within the accuracy of measurement, the oil OCP1H doesn't even show an increase of the film thickness compared to M100 at all. That is a consequence of the ability of the polymers SBC and OCP to form physical and chemical network structures. Those networks have a high thickening effect at standard conditions. At high pressure, temperature and shear rate, as in an EHL contact, however, those network structures are obviously not very stable and therefore lose a great part of their thickening power.

Figure 9 shows the measured film thicknesses of the test oils with polymers of high molecular weight and low concentration PIB2L, OCP2L, SBC2L, PMA2L, STAR-L and of the two mineral oils M100 and M240 at the same conditions as in Figure 8. None of the polymer-containing oils reaches the film thicknesses of the mineral oil M240 despite equal kinematic viscosities v_{100}. That is a consequence of the high molecular weight of those polymers, which causes a high temporary viscosity loss under the influence of a shear field, as shown in Figure 3. As the viscosity of an oil in the inlet region of an EHL contact is decisive for the height of the film thickness and as the viscosities of the test oils containing long-chain polymers are reduced to some extent within the high shear field in the inlet region of the disk contact, those test oils form lower film thicknesses than expected according to their viscosity data gained at standard laboratory conditions.

Film Thickness Calculation

Film Thickness Calculation in General. The lubricant film thicknesses h_{min} according to Dowson/Higginson (Ref. 5) and h_0 according to Ertel/Grubin (Refs. 6 and 8) in an EHL contact can be calculated for line contact condition as follows:

$$h_{min} = 2.65 \cdot R \cdot G^{0.54} \cdot U^{0.7} \cdot W^{-0.13} \quad (3)$$

$$h_0 = 1.95 \cdot R \cdot (G \cdot U)^{0.73} \cdot W^{-0.09} \quad (4)$$

The nondimensional EHL parameters G, U and W in the above equations are defined as:

$$G = \alpha \cdot E' \quad (5)$$

$$U = (\eta_M \cdot v_\Sigma)/(2 \cdot R \cdot E') \quad (6)$$

$$W = 2 \cdot \pi \cdot [(p_H/E')^2] \quad (7)$$

The reduced Young's modulus E' and the reduced radius of curvature R are calculated as follows:

$$E' = 2[(1-\nu_1^2/E_1) + (1-\nu_2^2/E_2)]^{-1} \quad (8)$$

$$R = (r_1 \cdot r_2)/(r_1 + r_2) \quad (9)$$

According to Murch/Wilson (Ref. 12), the accuracy of film thickness calculation can be improved by thermal correction, which takes into account the temperature rise of the oil in the inlet region of the contact, the rise being caused by the backflow of the surplus oil.

$$h_{min,\,thermal} = h_{min} \cdot C \quad (10)$$

$$h_{0,\,thermal} = h_0 \cdot C \quad (11)$$

with

$$C = 3.94/(3.94 + L^{0.62}) \quad (12)$$

$$L = (\eta_M \cdot \alpha_t \cdot v_\Sigma^2)/(4 \cdot \lambda) \quad (13)$$

$$\alpha_t = \ln(\eta_{40°C}/\eta_{100°C})/60K \quad (14)$$

Modification of Film Thickness Calculation for Polymer-Containing Oils. As the film thickness measurements prove, polymer-containing oils hardly ever form film thicknesses as high as a straight mineral oil of equal viscosity. That means that the usual kinematic viscosity, which is determined in a capillary viscometer at standard conditions, is not sufficient as an indicator for the film thicknesses to be expected for polymer-containing oils. As the usual film thickness calculation methods according to Dowson/Higginson (Ref. 5) or Ertel/Grubin (Refs. 6 and 8) include only the standard laboratory viscosity data, deviations between calculated and actual film thicknesses cannot be avoided for polymer-containing oils.

An improvement of the accuracy of film thickness calculation for polymer-containing oils requires modifying the calculation equations with a factor that correctly reflects the effective viscosity increase of polymers in an EHL contact. Polymer-specific properties, such as type, concentration or molecular weight of the polymers, cannot be used for such a factor, because those properties are usually not available to the user.

So a nondimensional polymer-correction factor P was derived from the film thickness test results. The factor takes into account the viscosity loss of a polymer-containing oil after a KRL-shear test. This term seems to be apt to specify the efficiency of polymers in an EHL contact, as the measurements showed a good correlation of high viscosity losses after a KRL-shear test with poor film thickness performance and vice versa. Besides, the KRL-shear test is a common and simple test method and its test devices are available in many laboratories.

The polymer-correction factor, which was derived from the test results, is defined as:

$$P = (\nu_{100,\,KRL}/\nu_{100,\,fresh})^{0.7} \qquad (15)$$

The exponent 0.7 in the above equation was chosen with respect to the weighting of the dynamic viscosity η in the usual film thickness equations.

The polymer-correction factor P is used to calculate the film thickness of polymer-containing oils as follows:

$$h_{min,\,thermal,\,pol.} = h_{min,\,thermal} \cdot P \qquad (16)$$

$$h_{0,\,thermal,\,pol.} = h_{0,\,thermal} \cdot P \qquad (17)$$

Those equations can, of course, also be used to calculate the film thickness of straight mineral or synthetic oils. In this case, the polymer-correction factor equals 1, because polymer-free oils practically don't lose any viscosity during a KRL-shear test. So the correction factor P is universally applicable for all lubricating oils.

The improvement of the accuracy of film thickness calculation by using the polymer-correction factor P is shown in Figures 10–13.

In Figure 10, the film thicknesses $h_{0,thermal}$, which were calculated without the polymer-correction factor P, are plotted against the measured film thickness-

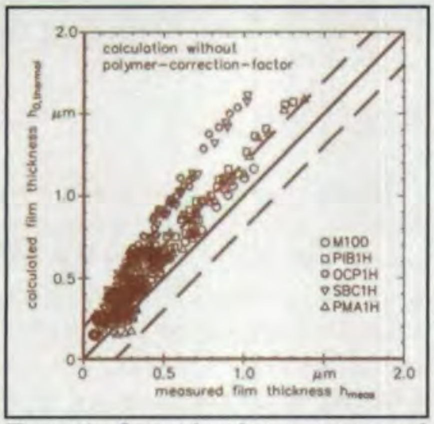

Figure 10—Comparison between measured and calculated film thicknesses of test oils ... 1H without polymer-correction factor.

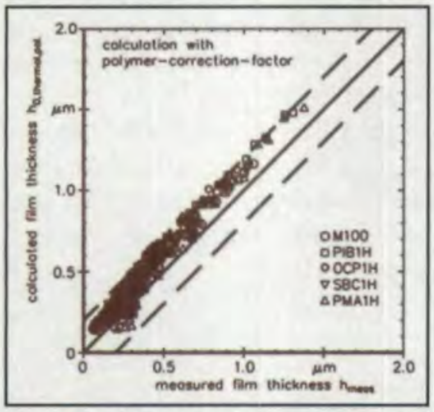

Figure 11—Comparison between measured and calculated film thicknesses of test oils ... 1H with polymer-correction factor.

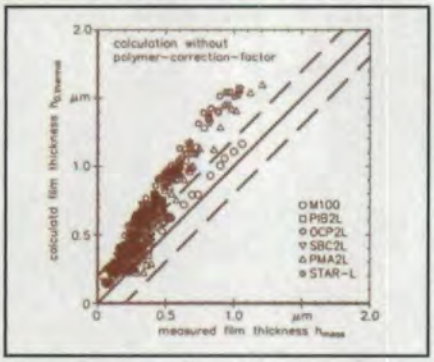

Figure 12—Comparison between measured and calculated film thicknesses of test oils … 2L without polymer-correction factor.

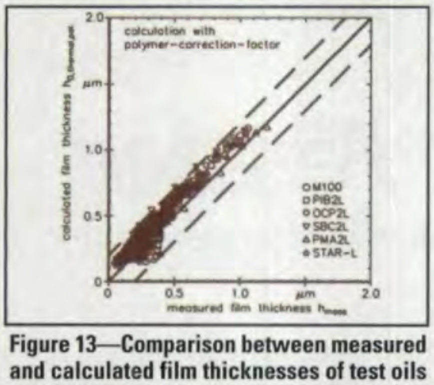

Figure 13—Comparison between measured and calculated film thicknesses of test oils ... 2L with polymer-correction factor.

es h_{meas} of the test oils …1H. All film thickness measurements at all conditions that had been carried out were regarded. The calculation overestimates the film thicknesses of the polymer-containing oils, especially those of SBC1H and OCP1H. For the polymer-free base oil M100, there is already a good correlation between measured and calculated film thicknesses. When modifying the calculation with the polymer-correction factor *P*, the accuracy of film thickness prediction improves considerably, as can be seen in Figure 11, where measured and calculated film thicknesses correlate quite well within the marked scatter range of ± 0.2 μm, even for the polymer-containing oils. For the majority of the measurements, the calculated film thicknesses are still slightly higher than the measured ones. That is a consequence of the difference between the bulk temperature ϑ_M, which is measured 2 mm below the disk surfaces and used for film thickness calculation, and the actual—slightly higher—temperature in the inlet region of the EHL contact. So the actual viscosity in the inlet region of the contact and thus also the actual film thickness are slightly lower than calculated.

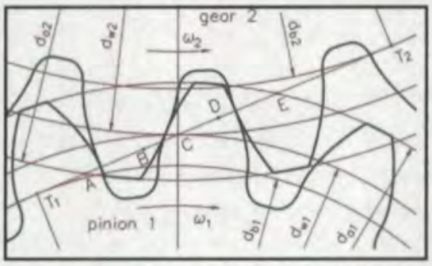

Figure 14—Line of contact of C-PT-type gears.

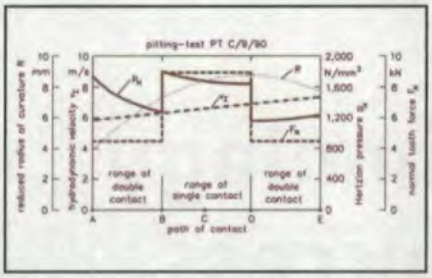

Figure 15—Some gear-specific parameters along the path of contact.

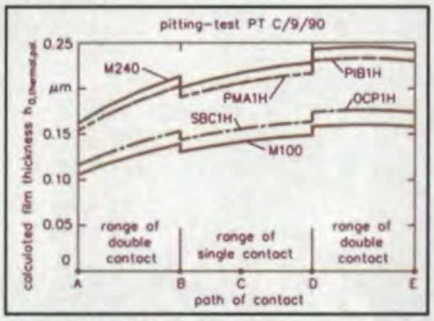

Figure 16—Calculated film thicknesses of test oils … 1H at pitting-test conditions.

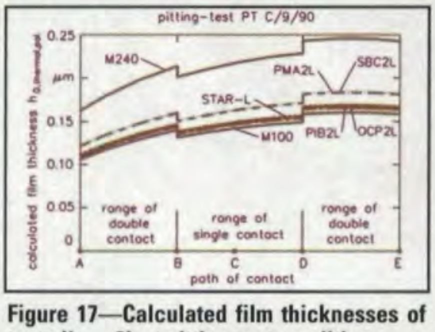

Figure 17—Calculated film thicknesses of test oils …2L at pitting-test conditions.

The use of applying the polymer-correction factor *P* to film thickness calculation for oils containing long-chain polymers is shown in Figures 12 and 13. The test oils …2L with long-chain polymers suffer from a high temporary and permanent viscosity loss by shearing. Using the polymer-correction factor *P* leads to a considerable improvement of the accuracy of film thickness calculation for the polymer-containing oils.

Altogether, the proper applicability of the polymer-correction factor *P* has been checked with approximately 3,000 film thickness measurements with 32 different polymer-containing oils, and it provided good results.

Application of the Modified Film Thickness Calculation to Gear Contacts. Figure 14 shows the line of contact of a C-PT-type spur gear pair as it is used for the standard pitting test PT C/9/90 (Ref. 7). Pinion 1 has 16 teeth, gear 2 has 24 teeth and the module is 4.5 mm. The base circles d_{b1} and d_{b2}, the pitch circles d_{w1} and d_{w2} and the tip circles d_{a1} and d_{a2} are shown in Figure 14 as well. The path of contact is limited on the line of contact by the beginning A and end E of contact. The points B and D represent the beginning and end of the range of single contact. C is the pitch point. The line of contact touches the base circles in points T_1 and T_2.

For calculating the lubricant film thickness within a gear contact, the distributions of the reduced radius of curvature R, the hydrodynamic velocity v_Σ and the Hertzian pressure p_H along the path of contact need to be known. As an example, those parameters are shown in Figure 15 for a C-PT-type gear pair and for the conditions of the standard pitting-test PT C/9/90. The reduced radius of curvature R forms a parabola along the line of contact, which equals 0 in T_1 and T_2. The hydrodynamic velocity v_Σ increases linearly from A to E. For the calculation of the Hertzian contact pressure, the normal tooth force F_N was assumed to be 100% in the range of single contact and to be 50% in the range of double-tooth contact. That is a simplification, which does not consider dynamic tooth forces. If the course of dynamic tooth forces along the path of contact is known by measurement or by calculation, the Hertzian contact pressure can be calculated more accurately.

With that gear data, the film thickness can be calculated along the path of contact of a gear mesh. An example is shown in Figure 16. The film thickness $h_{0,thermal,pol}$, which was calculated according to Ertel/Grubin (Refs. 6 and 8), with thermal correction according to Murch/Wilson (Ref. 12) and polymer-correction factor P, is plotted against the path of contact of a C-PT-type gear pair for the conditions of the standard pitting-test PT C/9/90 for the test oils with short-chain polymers and high concentrations. The relevant tooth bulk temperature was assumed to be constant at 100°C. Without using the polymer-correction factor P, the film thicknesses of all polymer-containing oils would be calculated equal to that of M240. Using the polymer-correction factor P, the calculated film thicknesses of the polymer-containing oils represent the actually measured values better (see Fig. 8).

Another calculation example in Figure 17 shows the film thicknesses of the test oils ...2L with the long-chain polymers in low concentration. Again, calculation would provide film thicknesses equal to M240 for all polymer-containing oils without using the polymer-correction factor. With the factor, the calculated film thicknesses show much better correlation with the measured ones (see Fig. 9).

Summary

The lubricant film thicknesses of a number of polymer-containing oils and their base oils were measured systematically in a twin-disk test rig. The investigated polymers were polyalkylmethacrylates (PMA), polyisobutylenes (PIB), olefin copolymers (OCP), styrene butadiene copolymers (SBC) and star-shaped styrene isoprene copolymers (STAR), each with two different molecular weights. In addition, the base oil viscosity and the concentration of the polymers in the base oil were varied. For information about the shear-stability of the polymers, the temporary and permanent viscosity loss by shearing were determined separately from each other by means of HTHS-viscosity measurements and KRL-shear-stability tests.

All polymer-containing oils formed lower film thicknesses than a straight mineral oil of the same kinematic viscosity v_{100} over a wide range of operating conditions. Short-chain polymers in high concentration in the base oil turned out to be significantly more effective in the contact than long-chain polymers in low concentration with the same viscosities. Polymers with thickening power mainly based on the formation of network structures, such as SBC, provided poor film forming properties. Those findings are in good accordance with the findings of other authors, for instance Professor Spikes (Refs. 11, 14 and 15) from the Imperial College in London, who carried out a great number of optical film thickness measurements with various polymer-containing oils.

A correction factor P was derived from the test results, by which the accuracy of film thickness calculation can be improved significantly for polymer-containing oils. The application of the correction factor is demonstrated and its practical use is exemplified by calculating the film thicknesses of some polymer-containing oils in a gear contact.

Acknowledgments

This research project was sponsored by the German Society for Petroleum and Coal Science and Technology (DGMK) in the German Federation of Industrial Cooperative Research Associations (AiF) by funds of the German Federal Ministry of Economics and Technology (BMWi).

References

1. Bartz, W.-J. "Bewertung des reversiblen und irreversiblen Viskositätsverlustes von Mehrbereichsölen," *Tribologie und Schmierungstechnik*, 41. Jahrgang, 4/1994, S. 214–218.

2. CEC L-45-A-99, "Viscosity Shear Stability Test Procedure for the Tapered Roller Bearing Test Rig," 1999.

3. CEC L-37-T-85, "Shear Stability of Polymer-Containing Oils (FZG Spur Gear Test Rig)," 1986.

4. DIN/ISO 2909, "Berechnung des Viskositätsindex aus der kinematischen Viskosität," July 1979.

5. Dowson, D. and G.R. Higginson, *Elastohydrodynamic Lubrication*, Oxford. Pergamon Press, 1966.

6. Ertel-Mohrenstein, A. "Die Berechnung der hydrodynamischen Schmierung gekrümmter Oberflächen unter hoher Belastung und Relativbewegung," *VDI-Fortschrittsbericht* Reihe 1, Nr. 115, 1984.

7. *FVA-Informationsblatt* zum Forschungsvorhaben Nr. 2/IV: "Pittingtest – Einfluß des Schmierstoffes auf die Grübchenlebensdauer einsatzgehärteter Zahnräder im Einstufen- und im Lastkollektivversuch," 1997.

8. Grubin, A.N. and J.E. Vinogradova, *Investigation of the contact machine components*, Cent. Sci. Res. Inst. Tech. Mech. Eng., Moscow, Book No. 30, 1949.

9. Kopatsch, F. "Systematische Unter-suchungen zum Einfluß von polymeren Zusätzen auf die EHD-Schmierfilmdicke," *DGMK-Forschungsbericht* Nr. 466-01, 1999.

10. Mann, U. "Messung von Schmierfilmdicken im EHD-Kontakt. Einfluß verschiedener Grundöle und Viskositäts-Index-Verbesserer," *DGMK-Forschungsbericht* Nr. 466, 1995.

11. Mitsui, H. and H.A. Spikes, "Predicting EHD Film Thickness of Lubricant Polymer Solutions," *Tribology Transactions*, Vol. 41, 1, 1998, pp. 1–10.

12. Murch, L.E. and W.R.D. Wilson, "A Thermal Elastohydrodynamic Inlet Zone Analysis," *Trans. ASME F, J. Lubr. Techn.* 97, 2, 1975, pp. 212–216.

13. Simon, M. *Messung von elasto-hydrodynamischen Parametern und ihre Auswirkung auf die Grübchentragfähigkeit vergüteter Scheiben und Zahnräder*, Diss. TU München, 1984.

14. Smeeth, M., H.A. Spikes and S. Gunsel, "The Formation of Viscous Surface Films by Polymer Solutions: Boundary or Elastohydrodynamic Lubrication?" *Tribology Transactions*, Vol. 39, 3, 1996, pp. 720–725.

15. Smeeth, M., H.A. Spikes and S. Gunsel, "Boundary Film Formation by Viscosity Index Improvers," *Tribology Transactions*, Vol. 39, 3, 1996, pp. 726–734.

Tell Us What You Think . . .

If you found this article of interest and/or useful, please **circle 312.**

If you did not care for this article, **circle 313.**

If you would like to respond to this or any other article in this edition of *Gear Technology*, please fax your response to the attention of Randy Stott, managing editor, at 847-437-6618 or send e-mail messages to *people@geartechnology.com.*

U.S. Postal Service Statement of Ownership, Management and Circulation As of September 30, 2001

Publication Title: Gear Technology, The Journal of Gear Manufacturing
ISSN No.: 0743-6858
Published: Bimonthly, 6 issues per year
Annual Subscription Price: $45.00
Mailing Address of Publication: 1425 Lunt Avenue, Elk Grove Village, Cook County, IL 60007
Name & Mailing Address of Publisher: Michael Goldstein, 1425 Lunt Avenue, Elk Grove Village, Cook County, IL 60007
Name & Mailing Address of Editor: Michael Goldstein, 1425 Lunt Avenue, Elk Grove Village, Cook County, IL 60007
Name & Mailing Address of Managing Editor: Michael Goldstein, 1425 Lunt Avenue, Elk Grove Village, Cook County, IL 60007
Name & Mailing Address of Owner: Michael Goldstein & Richard Goldstein, 1425 Lunt Avenue, Elk Grove Village, Cook County, IL 60007
Known Bondholders: None

Issue Date for Circulation Data Below: September/October 2001

Extent and Nature of Circulation	**Actual No. Copies of Single Issue Published Nearest to Filing Date**	**Average No. Copies Each Issue During Preceding 12 Months**
a. Total Number of Copies (Net press run)	14,482	14,036
b1. Paid/Requested Outside-County Mail Subscriptions, as Stated on Form 3541	9,527	9,467
b2. Paid In-County Subscriptions, as Stated on Form 3541	0	0
b3. Sales Through Dealers and Carriers, Street Vendors, Counter Sales and Other Non-USPS Paid Distribution	350	346
b4. Other Classes Mailed Through the USPS	0	0
c. Total Paid and/or Requested Circulation	9,877	9,813
d1. Free Distribution Outside-County, as Stated on Form 3541	2,551	1,470
d2. Free Distribution In-County, as Stated on Form 3541	0	0
d3. Free Distribution Other Classes Mailed Through the USPS	0	0
e. Free Distribution Outside the Mail	1,322	1,613
f. Total Free Distribution	3,873	3,083
g. Total Distribution	13,750	12,896
h. Copies Not Distributed	732	1,140
i. Total	14,482	14,036
j. Percent Paid and/or Requested Circulation	71.8%	76.1%

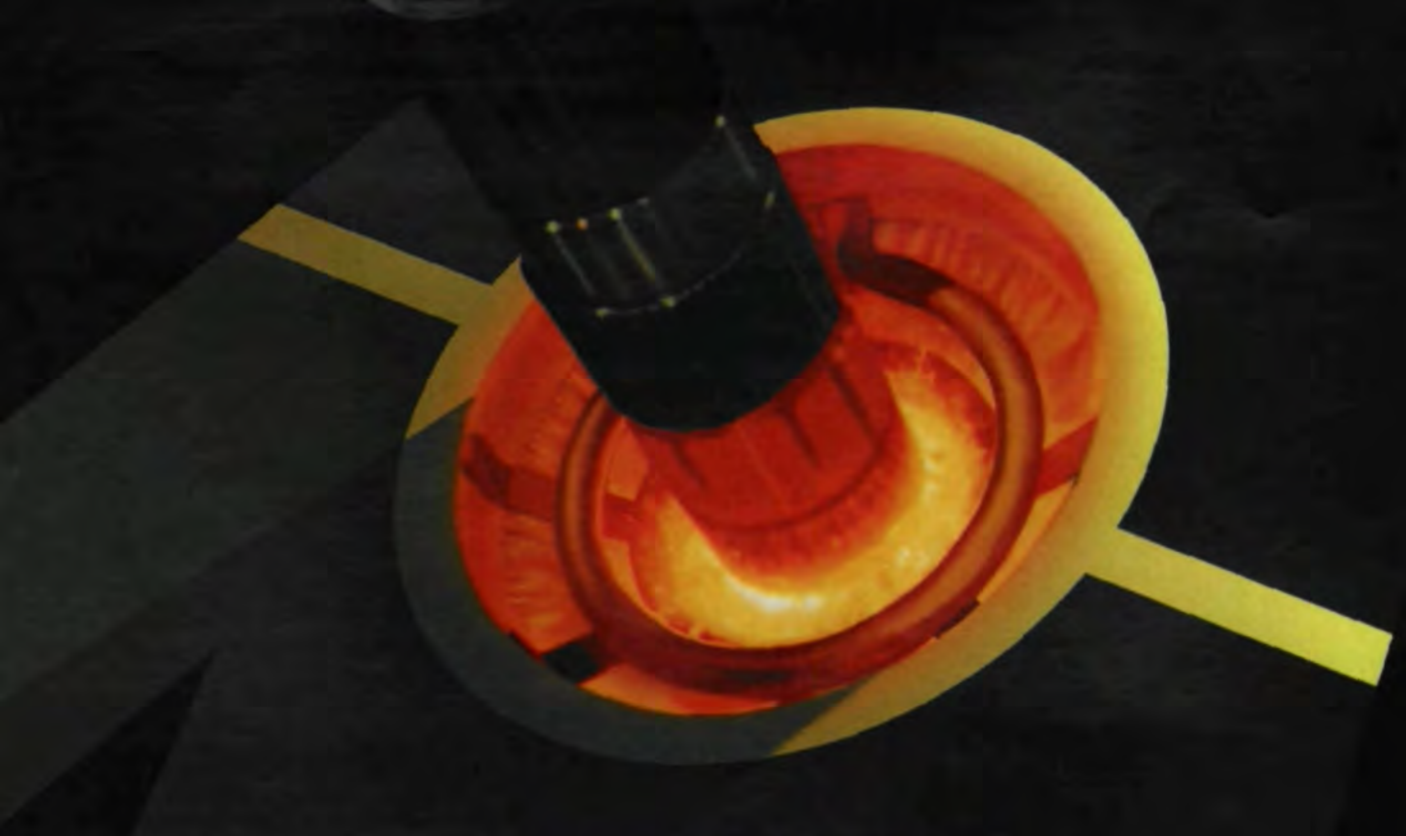

ADVERTISER INDEX

For more information about a product or service advertised in this issue of *Gear Technology*, circle the appropriate number on the Reader Response Card and put the card in the mail.

TRY OUR RAPID READER RESPONSE SYSTEM!
Go to *www.geartechnology.com/rrr.htm* to request additional information from any advertiser in this issue. Your request will be sent to the advertiser within 24 hours for super-fast turnaround!

ADVERTISER	READER SERVICE NUMBER	PAGE NUMBER
Ajax Magnethermic Corp.	117	40
American Metal Treating Co.	154	55
Applied Process	111	4
A/W Systems Co.	116	26
Barit International Corp.	136	39
Basic Incorporated Group		53
Bourn & Koch Machine Tool Co.	142	21
Crown Gear B.V.	144	21
Crucible Service Centers	119	52
Dr. Kaiser (S.L. Munson)	122	46
Dura-Bar	158	23
Expertech International	146	24
Fairfield Manufacturing Co. Inc.	123	49
Fässler Corp.	130, 171	35, 41
Forest City Gear	138	6
Frisby P.M.C. Inc.	155	55
The Gear Industry Home Page™	354	37
Gear Technology Center, Div. of Mitsubishi International Corp.	175	28–29
Gleason Cutting Tools Corp.	105, 156	BC, 55, 53
The Gleason Works	110	IFC–1, 53
Grupos Diferenciales S.A.	131	51
Hornet GmbH	157	55
Hydra-Lock Corp.	125	33
Index Technologies Inc.	160	54
Insco Corp.	147	17
Interstate Tool Corp.	162	54
ITW Heartland	127	45
Klingelnberg Söhne GmbH	103	10–11, 53
Koepfer America L.L.C.	172	55
Kreiter Geartech	163	54
LeCount Inc.	137	27
MicroGear	149	41
Midwest Gear & Tool Inc.	151	50
Midwest Gear Corp.	164	55
Nachi Machining Technology Co.	114	5
Niagara Gear Co.	166	54, 53
Parker Industries Inc.	152	17
Perry Technology Corp.	134	IBC
powertransmission.com™	355	52
Presrite Corp.	108	42
Process Equipment Co.	135	51
Pro-Gear Co. Inc.	168	54
The Purdy Corp.	129	38, 53
Raycar Gear & Machine Co.		53
Russell, Holbrook & Henderson	141	27
Sigma Pool		53
Star Cutter Co.	132, 169	2, 54
SU America Inc.	107	8
SUDA International Gear Works Ltd.	170	55
Toolink Engineering	153	24

Properties of Tooth Surfaces due to Gear Honing with Electroplated Tools

Carsten Marzenell and Hans Kurt Tönshoff

Introduction

In recent years, the demands for load capacity and fatigue life of gears constantly increased while weight and volume had to be reduced. To achieve those aims, most of today's gear wheels are heat treated so tooth surfaces will have high wear resistance. As a consequence of heat treatment, distortion unavoidably occurs. With the high geometrical accuracy and quality required for gears, a hard machining process is needed that generates favorable properties on the tooth surfaces and the near-surface material with high reliability.

Hard machining processes can modify properties such as surface roughness and topography, residual stress state, material structure and hardness in a wide range. From grinding, for instance, it is known that adverse process conditions may cause thermal overload that results in annealing zones, rehardening zones or even grinding burn. Those effects usually are characterized by the occurrence of high tensile residual stresses, as well as modifications of material structure and hardness in near-surface layers. Tensile residual stresses are especially regarded as causing cracks and crack growth. Consequently, a significant loss of fatigue life occurs. On the other hand, compressive residual stresses in near-surface layers have enhancing effects on fatigue life under dynamic load.

Different hard machining processes for gears were investigated at the Institute for Production Engineering and Machine Tools, at the University of Hannover, in Germany, to evaluate their effects on the properties of tooth surfaces. The emphasis of the results presented in this paper is based on the process of gear honing. That process's

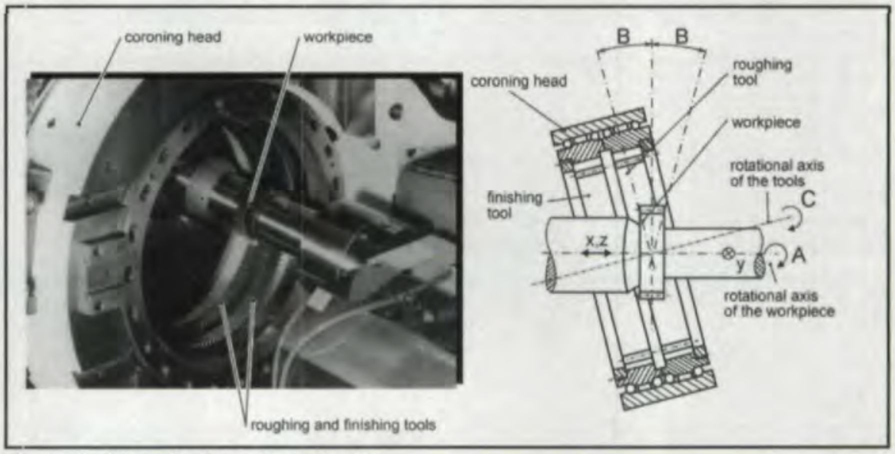

Figure 1—The principle of gear honing.

		m_n [mm]	z	β [°]	α_n [°]
gear	A	4.32	32	25	17.5
	B	4.32	31	24.8	17.5
	C	2.48	65	26	20
	D	3	45	15	20
	E	2	9	15	20

Figure 2—Geometries of investigated gears.

origin goes back to the 1970s, when Fässler AG of Dübendorf, Switzerland, first applied the kinematics of an internal geared tool meshing with an external geared workpiece. In the meantime, the process was adapted by several machine tool manufacturers and has gained increasing importance in the 1990s. In recent years, machine tool manufacturer Kapp GmbH of Coburg, Germany, developed the process of Coroning™, a power gear honing process with electroplated tools. The research work presented here is based on the Coroning process.

Gear honing includes several established terms, such as shave grinding, Coroning, power gear honing and spher-

Dr.–Ing. Carsten Marzenell

is a project manager with automotive supplier Robert Bosch GmbH of Stuttgart, Germany. He works in the assembly-systems & special-machinery department and specializes in the assembly of electronic throttle systems. From July 1995 to May 2000, he was a scientific collaborator at the Institute of Production Engineering and Machine Tools, at the University of Hannover, in Germany. He worked in the institute's production-processes department, where he specialized in gear machining, grinding, hard machining, and high-pressure water peening.

Prof. Dr.-Ing. Dr.-Ing. E. h. Hans Kurt Tönshoff

is head of the Institute for Production Engineering and Machine Tools.

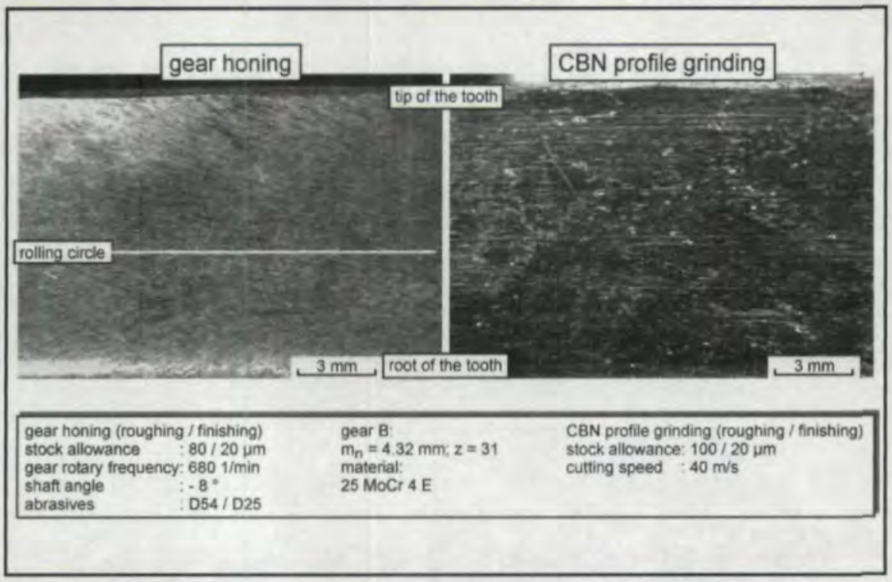

Figure 3—Machining groove lines due to gear honing and profile grinding.

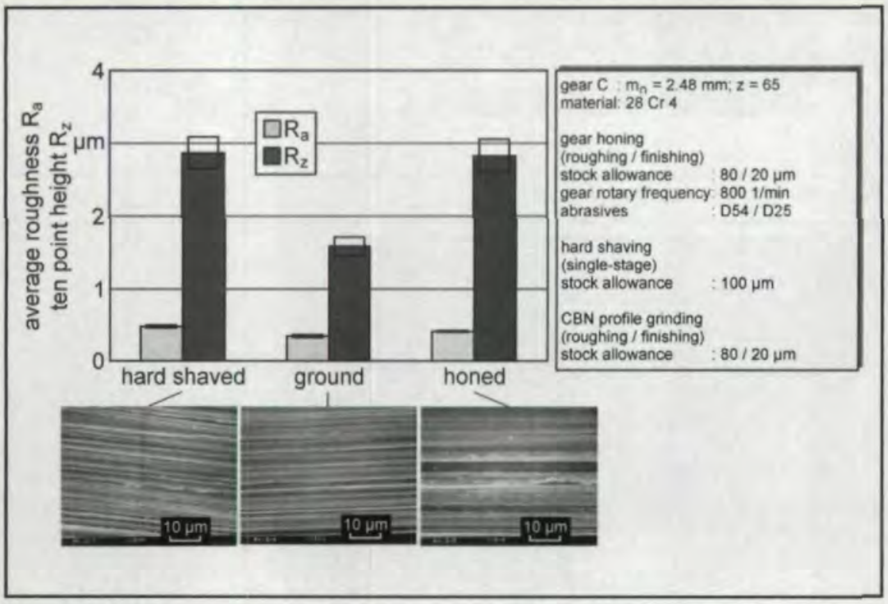

Figure 4—Surface roughness due to gear honing and alternative gear machining processes. The cutoff length was 5.6 mm.

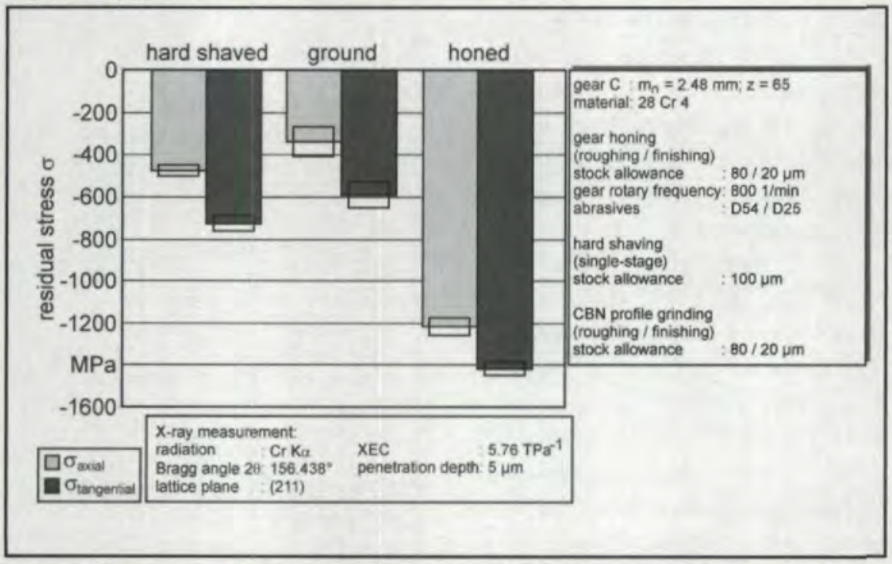

Figure 5—Residual stresses due to gear honing and alternative gear machining processes.

ic honing. Still, the expression "gear honing" will be used in this paper, as it is most widely used.

Machine Tool Concept and Process Characterisitics

All experiments on gear honing were performed on a Coroning machine VAC 65, manufactured by Kapp GmbH. The machine tool offers two spindles for the workpiece (A-axis) as well as for the tools (C-axis). Each spindle has a nominal power of 14 kW and enables rotary frequencies up to a maximum of 800 1/min. Gears up to tip diameters of 220 mm, maximum modules of 6 mm, maximum widths of 80 mm and maximum workpiece lengths of 500 mm can be machined in the working area.

Gear honing on the Coroning machine VAC 65 removes maximum stock allowances of 130 µm on the gear flanks. No premachining process is necessary after heat treatment. The heat-treated workpiece, whose permissible hardness is limited to 62 HRC, undergoes a roughing operation and a following finishing operation. The principle of gear honing and the working area of the machine tool are shown in Figure 1. The kinematics is based on the continuous meshing of an internal geared tool with the workpiece to be machined. During gear honing, the axes of the tool and the workpiece have a defined shaft angle that results in material removal because of the relative motion between the flanks of the tool and the workpiece.

A roughing tool and a finishing tool are mounted in the Coroning head. The tools represent internal geared metallic bodies whose tooth flanks are electroplated with a single layer of abrasives. In our experiments, diamond grit of the specification D54 (roughing tool) and D25 (finishing tool) was used. During tool life, no dressing operations are necessary. When the tools are worn, the abrasives are removed from the metallic body and a new layer of diamond grit can be applied.

To enable reduction of the pitch error during gear honing, the axes of the workpiece and the tools are electronically coupled via control of the machine tool.

The gears used for the presented

experimental research work are shown in Figure 2. Gears A and B, with a large module of 4.32 mm, are made of case hardened 25MoCr4 steel and built for truck gearboxes. Gear C, with a significantly smaller module of 2.48 mm, is a part of differential gearboxes for passenger cars and consists of tempered 28Cr4 steel. Gears D and E run in stationary gearboxes and are made of case hardened 16MnCr5 steel.

To evaluate the properties of the gears machined experimentally, residual stress state, surface roughness, surface topography, material structure and microhardness were investigated. The residual stress analysis was performed on an X-ray diffractometer using CrKa radiation. In order to obtain depth profiles of residual stresses, surface layers of tooth flanks were removed in several steps by electrolytic polishing. This process guarantees the absence of thermal and mechanical loads that would modify the residual stress state. After polishing, residual stress measurement was carried out in the determined depth before the cycle of polishing and measuring began afresh.

For roughness measurements, a contact stylus instrument Perthometer Concept was used. Photographs of the surface topography were taken by light-optical and scanning electron microscopy. Effects on hardness and material structure were detected by photographs of metallographic preparations and microhardness measurements. The most interesting results of the investigations on honed gear tooth flanks are presented in the following paragraphs.

Surface Roughness and Topography

The kinematics in gear honing is characterized by the meshing of the gear to be machined with the internal geared tool under a shaft angle. As a consequence, the relative motion between the tool and the workpiece is composed of a roll and a screw movement (Ref. 4). With a shaft angle of 0°, a mere roll movement occurs. But, a shaft angle different from 0° results in a screw component that causes an additional slide movement in tip-root direction. With regard to the single grain contact in gear honing, curved groove lines occur that are not parallel to the tooth trace. Figure 3 presents a comparison of typical surface structures generated by gear honing and CBN profile grinding. The microscopic photographs show tooth flanks of gear B, which were machined alternatively by the two processes.

Due to the axial feed direction of the grinding wheel, the ground tooth flank shows straight-lined grooves that are parallel to the tooth trace. In gear honing, machining grooves are only parallel to the tooth trace near the pitch circle. In the areas near the tip and the root, the directions of the machining grooves and the tooth trace include a cutting angle that increases as the distance from the pitch circle increases.

Besides the structures of the surfaces generated by different gear machining processes, surface roughness was also investigated. Samples of gear C were machined by gear honing, hard shaving or CBN profile grinding. Though shaving is a soft machining process in most cases, hard shaving is an application suitable for hardened gears.

The roughness values after machining are compared in Figure 4. Lowest ten point height values of only 1.6 µm were measured at the ground variant. Gear honing and hard shaving led to comparatively higher ten point height values between 2.6 and 3.1 µm.

In Figure 4, the surface roughness for honing may seem high. That is due in part to a misnomer. Gear honing with electroplated tools refers to a "honing" process, but it is actually a grinding process using a profiled grinding tool. The high roughness is also due in part to the tool specification.

Residual Stresses

The residual stress state plays an important role concerning fatigue life of components under dynamic load. In gear grinding, modification of the grinding conditions, such as increasing wear of the grinding wheel or varying cutting speeds, can cause residual stresses that widely vary from tensile to compressive range (Ref. 1). Tensile residual stresses are regarded as causing cracks and forcing crack growth. On the other hand, compressive residual stresses in near-surface layers have enhancing effects on fatigue life under dynamic load. Therefore, the interactions between different hard machining processes and the residual stress states generated are of high importance.

To investigate those interactions, machining of gear C was done by the three competing processes of hard shaving, CBN profile grinding and gear honing. The residual stresses measured at the surface of tooth flanks in axial and tangential directions are displayed in Figure 5. One can see that all of the mentioned processes induce compressive residual stresses. The lowest compressive residual stresses were found after profile grinding. Hard shaving induces slightly higher compressive stresses between –474 MPa and –729 MPa. But the highest compressive residual stresses occur due to gear honing. Depending on the direction of measurement, they range from –1,217 MPa to –1,419 MPa.

Similar investigations were done for gear B, which was machined by gear honing and CBN profile grinding. In this case, compressive residual stresses between –1,031 MPa and –1,304 MPa were detected after gear honing. As for grinding, lower compressive stresses of around –900 MPa could be measured.

When discussing those high compressive residual stress states after machining, the question arises whether the stresses were generated by machining or were already in the material due to the preceding heat treatment. To clarify that, residual stresses states after case hardening and after the roughing and finishing operations of gear honing were investigated. The investigations were done on gear A. Figure 6 shows a comparison of the depth profiles of residual stress obtained after case hardening as well as after roughing and finishing. Directly at the surface of the unmachined part, high compressive residual stresses of about –850 MPa occur. The maximum compressive residual stress was found at a depth of 10 µm. Because the roughing operation in gear honing removes a stock allowance of 80 µm (light grey area in the diagram), compressive residual stresses in those layers are of no importance. The surface generated by the roughing operation is equivalent to a depth of 80 µm, where the unmachined part shows only low compressive residual stresses of about –455 MPa.

In the diagram, the surface generated by roughing lies at a depth of 80 µm. The depth profiles of residual stress induced by roughing are marked by the dotted lines. High compressive residual stresses occur directly at the roughened surface. Dependent on the direction of measurement, they range from –1,026 MPa to –1,315 MPa. Compared to the initial state of the material (continuous lines), one can see an increase in compressive residual stresses of more than 600 MPa induced by the roughing operation in gear honing.

After roughing, the maximum compressive residual stress was found at the surface of the tooth flank. But a significant increase of compressive residual stress was also detected below the surface. The influencing of the residual stress state due to roughing reaches material regions up to depths of almost 40 µm.

As the finishing operation removes an additional stock allowance of 20 µm (dark grey area), the surface of the finished workpiece can be found at a depth of 100 µm, and the residual stress profiles after finishing are marked by the dashed lines. Again, the maximum compressive residual stress occurs at the surface, although the values between –968 MPa and –1,245 MPa are slightly lower than after roughing. The compressive residual stresses could be increased up to depths of about 30 µm.

High compressive residual stresses can be attributed to the high mechanical

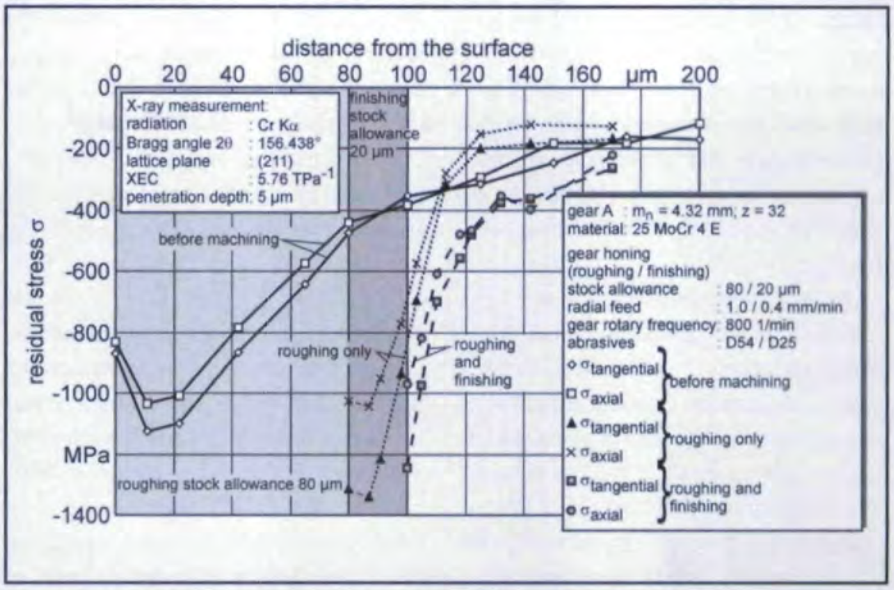

Figure 6—Depth profiles of residual stress after different production steps.

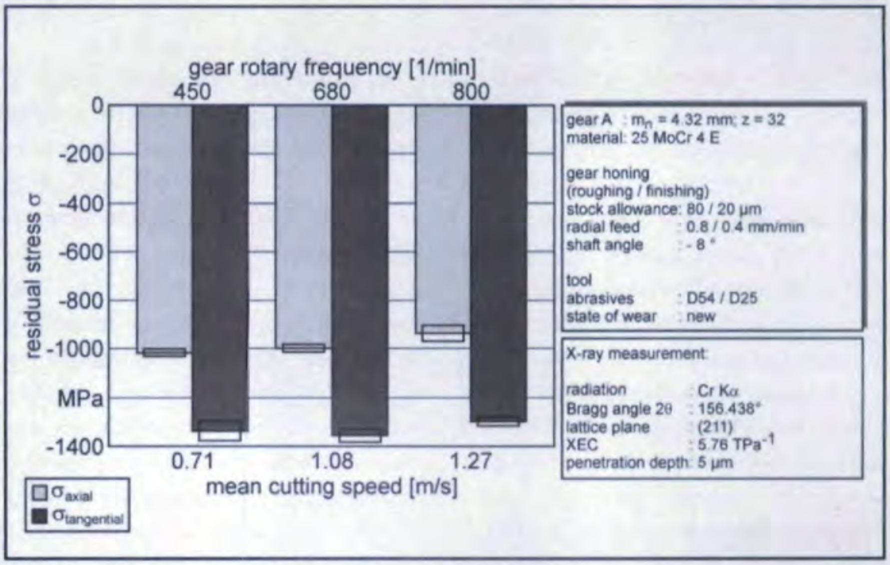

Figure 7—Residual stresses due to different cutting speeds.

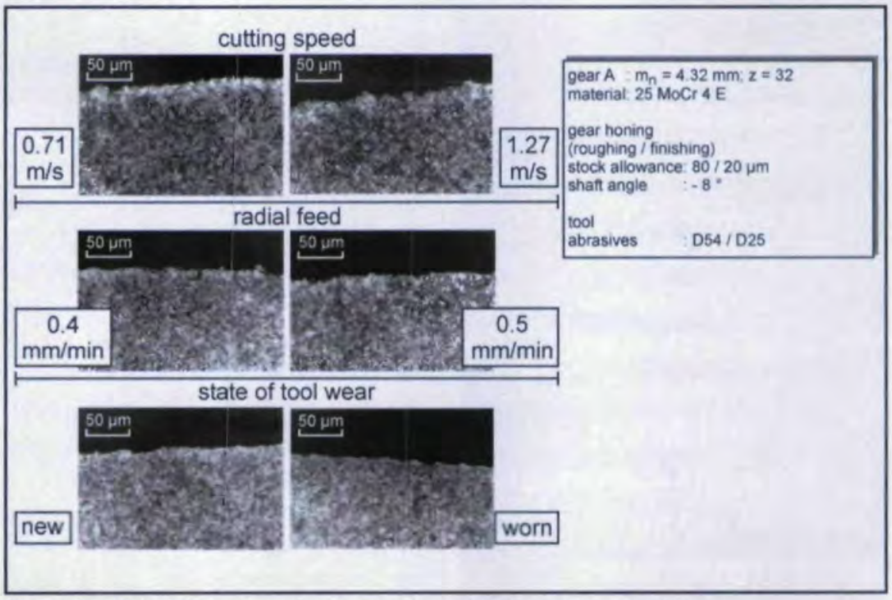

Figure 8—Material structure due to gear honing under various conditions.

forces in gear honing caused by machining with superhard diamond abrasives. In roughing, the machining forces are higher due to using the coarser diamond grit D54, which is why the increase in compressive residual stress and the effect on depth are higher than in finishing with D25 grit.

It has become apparent that gear honing with electroplated diamond tools leaves high compressive residual stresses in the near-surface material. Admittedly, the interactions between process layout of gear honing and the induced residual stresses had to be discovered. For that reason, gear honing experiments with varying cutting speeds were carried out using gear A as the workpiece. The variation of the cutting speed was realized by changing the workpiece rotary frequency. Figure 7 displays surface residual stresses dependent on different mean cutting speeds and gear rotary frequencies.

Cutting speeds of 0.71, 1.08 and 1.27 m/s were used, which correspond with rotary frequencies of 450, 680 and 800 1/min. For all mentioned conditions, high compressive residual stresses occur in axial and tangential direction. While no variations of residual stresses can be stated for cutting speeds of 0.71 and 1.08 m/s, a slight decrease was found for a cutting speed of 1.27 m/s. Measurements of the spindle's consumption showed a decrease with increasing rotary frequency. That indicates that lower machining forces can explain the slight decrease in compressive residual stresses when using high cutting speeds.

WHEREAS PRODUCTIVE EFFICIENCY OF GEAR HONING IS AT LEAST IN THE RANGE OF GEAR GRINDING, THE GEAR HONING PROCESS ALSO EFFECTS FAVORABLE PROPERTIES IN THE TOOTH FLANKS.

Structural Modifications

The generation of material properties when machining with geometrical, undefined cutting edges is always caused by the interaction of mechanical and thermal loads in the contact zone. While mechanical forces can induce compressive residual stresses that strengthen the material, the occurrence of high thermal loads shifts residual stresses to the tensile range and causes structural modifications, such as annealing zones or even rehardening zones, so-called white layers. Even though the phenomenon of white layers is not completely investigated yet, their formation is regarded as harmful to the workpiece (Ref. 1).

In gear honing, the already described generation of high compressive residual stresses can be attributed to strong mechanical forces. Thermal loads obviously play a minor role. That assumption is stressed when one takes into consideration the influence of cutting speeds in gear honing. In general, the amount of thermal load increases when using higher cutting speeds. Whereas in grinding gear B, a cutting speed of 40 m/s was used, the mean cutting speed in honing of the same gear geometry only amounts to about 1 m/s, which indicates low thermal influencing of the near-surface material.

To finish evaluating the thermal effects in gear honing, modifications of the material structure near the surface were investigated. Figure 8 shows microscopic photographs of near-surface structures due to gear honing under completely different conditions.

Variations of the cutting speed, the radial feed and the state of tool wear were used in the gear honing experiments to create favorable and adverse process conditions. The three photographs on the left side display the structures generated as a consequence of favorable process conditions with lowest thermal loads possible. Near the surface, no structural modifications can be seen.

The process conditions used for the specimens on the right side were chosen to create high temperatures in the contact zone. Gear honing with worn tools effects high friction, which results from the low cutting ability of the diamond grits' blunt and rounded cutting edges. A high cutting speed of 1.27 m/s also causes increasing friction. In spite of high thermal loads due to increased friction, the photographs on the right side show no modifications of the structure at all. Effects like annealing zones or rehardening zones can be avoided with high reliability. Those discoveries are stressed by additional microhardness measurements, which were performed on the discussed specimens. In all cases, no alterations of the microhardness due to gear honing could be measured. Those facts indicate that, in contrast to grinding, the temperatures in gear honing are too low to cause thermal damage even under the most unfavorable process conditions.

Conclusions

For ecological and economic reasons, the demands for fatigue life and load capacity of gears constantly increase. Under aspects of low development costs and risk, the design of gears often remains unchanged and the improved performance of the product has to be achieved by better quality due to improved and efficient manufacturing processes. In recent years, the process of gear honing with electroplated tools has been established as a competitive finishing process for hardened gears. In contrast to conventional gear honing with corundum tools, high stock allowances up to 130 μm can be removed, and premachining processes after heat treatment can be abolished.

Whereas productive efficiency of gear honing is at least in the range of gear grinding, the gear honing process also effects favorable properties in the tooth flanks. Surface structures with curved groove lines are generated. The surface roughness due to gear honing is slightly higher compared with competing gear machining processes. One further advantage of gear honing with electroplated tools is the generation of high compressive residual stresses directly at the surface, as well as in the near-surface material. Compressive residual stresses are regarded as a means of preventing cracks and stopping crack growth under cyclic load and therefore increase fatigue strength. In gear honing, the compressive residual stress states can be reproduced with very high reliability. Even when varying the cutting speed or the workpiece rotary frequency respectively, almost the same stress states occur.

The cause for high compressive residual stresses was found in the combination of mechanical and thermal loads in gear honing. On the one hand, high mechanical forces that strengthen the material emerge from machining with superhard abrasives. On the other hand, very low cutting speeds in the range of 1 m/s result in low process temperatures. Therefore, unfavorable shifting of the residual stresses to tensile range as well as modifications of the near-surface material structure are avoided with high reliability.

Acknowledgments

The scientific work presented in this paper results from a cooperative research project with the Institute for Production Engineering and Machine Tools, Hannover, and the companies Kapp GmbH, Coburg; Daimler-Benz AG, Gaggenau; Ford-Werke AG, Köln; and Lenze GmbH & Co KG, Extertal. The project was financed by the German Federal Ministry for Education and Science and supported by Research Centre Jülich.

References

1. Tönshoff, H.K., B. Karpuschewski and C. Marzenell, "Surface generation by hard machining," *Proceedings of the Fourth European Conference on Residual Stresses*, Vol. 1, Cluny en Bourgogne, June 4–6, 1996, p. 13–31.

2. Tönshoff, H.K., I. Inasaki, B. Karpuschewski, and Th. Mandrysch, "Grinding process achievements and their consequences on machine tools—challenges and opportunities," *CIRP Annals* 1998, Volume 47/2/1998, Verlag Technische Rundschau, Berne, Switzer-land, 1998.

3. Tönshoff, H.K., B. Karpuschewski, and F. Werner, "Prozeßnahe Qualitätssicherung in der Feinbearbeitung," *Proceedings of the 7. Internationales Braunschweiger Feinbearbeitungskolloquium (FBK)*, Braunschweig, March 2–4, 1993, p. 3.01–3.19.

4. Brinksmeier, E., U. Berger and Ch. Schneider, "Technologische Nachbildung des Schabschleifens (Verzahnungshonen)," *Jahrbuch Schleifen, Honen, Läppen und Polieren*, Volume 58, edited by H.K. Tönshoff and E. Westkämper, Vulkan-Verlag Essen, 1996.

5. Gosdin, M. "Neues Verfahren für die Hartfeinbearbeitung von Zahnrädern in großen Serien," *Industrial Diamond Review* 1 (1994), p. 15–17.

6. Bausch, Th., "Verfahrensmerkmale beim Schleifen und Honen von Zahnrädern, Part II," *Industrial Diamond Review* 2 (1994), p. 94–98.

This paper was originally presented at the 4th World Congress on Gearing and Power Transmission in Paris, March, 1999.

Tell Us What You Think . . .

If you found this article of interest and/or useful, please **circle 314.**

If you did not care for this article, **circle 315.**

If you would like to respond to this or any other article in this edition of *Gear Technology*, please fax your response to the attention of Randy Stott, managing editor, at 847-437-6618 or send e-mail messages to *people@geartechnology.com.*

Mahr Federal Upgrades PRIMAR

Mahr Federal Inc. added a new 3-axis gagehead and application family software to its PRIMAR universal measuring system.

Mahr Federal said that the gagehead's 3-D maneuverability assures the probe is always normal to the measurement surface for minimal deflection and that the probe can continuously scan up to 19,200 measurement points for nonprismatic dimensional characteristics, as well as roundness and diameter.

For more information, contact Mahr Federal of Providence, RI, by telephone at (800) 969-1331, by fax at (513) 489-6302, by e-mail at *info@fedprod.com*, or on the Internet at *www.mahrfederal.com* or *www.mahr.com*.

Circle 350

New Gear Roundness Measuring System from Mitutoyo

Mitutoyo America Corp. has a new roundness measuring system for gears and various cylindrical forms: the RA-H5000.

In its press release, Mitutoyo said its system offers high accuracy and production speed, fully automates measurement, assessment and printout of gears and cylindrical forms, and much improves throughput, measuring accuracy and analysis performance.

The system has a turntable rotational accuracy of (0.02 + 6H/10,000)mm, vertical column straightness of 0.05 mm/100 mm, parallelism with rotating axis of 0.2 mm/350 mm and measuring arm straightness of 0.5 mm/200 mm.

For more information, contact Mitutoyo, located in Aurora, IL, by telephone at (630) 978-5385, by fax at (630) 820-7403, by e-mail at *info@mitutoyo.com*, or on the Internet at *www.mitutoyo.com*.

Circle 351

New CNC Automatic Lathes from Meritage

Two new CNC precision automatic lathes that can hob gears are available through REM Sales Inc., a division of Meritage Inc. The new lathes are the Tsugami MU 26/38 and BU 26/38, two Swiss-style machines.

In its press release, Meritage said the machines have the largest bar stock capacity of any Swiss-style machines in their class. The models can accommodate bar stock up to 38 mm in diameter, with stroke of 250 mm, main spindle output of 11/7.5 kW and sub side output of 5.5/3.7 kW. The models are available with either 26 mm or 38 mm bar stock capacity.

Meritage said those configurations permit high-precision complex thread milling, polygon machining, gear hobbing and balanced turning and threading.

For more information, contact REM Sales, located in East Granby, CT, by telephone at (860) 653-0071, by fax at (860) 653-0393, or by e-mail at *sales@remsales.com*.

Circle 352

New Gear Hobbing Machine from Hamai

Hamai Co. Ltd. has a new CNC 5-axis gear hobbing machine that can cut wet or dry, can reach a hob spindle speed of 5,000 rpm and can direct cut heat-treated gears of 50 HRC.

The machine, N-60, can cut up to module 2 and an outside diameter of 100 mm, and has a FANUC 18MC CNC control with five axes.

In its press release, Hamai Co. Ltd. of Tokyo, Japan, said the machine was simple to operate with its conversational-type cutting data input system.

For more information, contact Hamai by e-mail at *k-sato@hamai.com*, by fax at (81) 3-3494-7536, or on the Internet at *www.hamai.com*.

Circle 353

Tell Us What You Think . . .

If you found this column of interest and/or useful, please **circle 357.**

If you did not care for this column, **circle 358.**

If you would like to respond to this or any other article in this edition of *Gear Technology*, please fax your response to the attention of Randy Stott, managing editor, at 847-437-6618 or send e-mail messages to *people@geartechnology.com*.

CIRCLE 135

CIRCLE 131

WEBFINDER MART

ADVERTISING SECTION

Companies listed below offer product information and design assistance on the World Wide Web. Reach them through home pages listed below.

GLEASON CUTTING TOOLS CORPORATION

Gleason Cutting Tools Corporation is the leading gear cutting tool manufacturer in North America. We offer a wide variety of form-relieving milling cutters, hobs, shaper cutters, shaving cutters and CBN-plated form grinding wheels as well as our engineering, coating, heat treating, metallurgical, tool sharpening and reconditioning services.

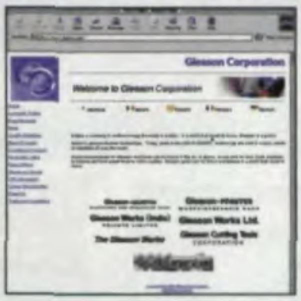

www.gleason.com

GLEASON

Gleason is the world's most comprehensive resource for gear manufacturing technology. We offer a comprehensive gear cutting machine program for every gear hobbing, milling and grinding application for cylindrical and bevel gears. To learn more about our products and services or to find key contact information, see our Web site.

www.gleason.com

BASIC MACHINE TOOLS

• Machine tool experience since 1937 • Distribution of Gear machines since 1951 • Broad inventory of NEW Gear machines • Offering 39 models of gear hobbing machines, 13 models of gear shaping machines and 30 models of other gear machines • The only major source of many NEW "manual" gear machines • Some "CNC" machines also available

www.basicmachinetools.com

NIAGARA GEAR

The Niagara Gear Website details our precision ground spur, helical and pump gears. All our gears are manufactured with the latest gear grinding technology. The web site also provides information on Niagara Gear's complete capabilities to meet your most demanding, close tolerance requirements with fast turnaround.

www.niagaragear.com

RAYCAR GEAR & MACHINE CO.

Raycar is a privately owned company that manufactures many types of gears. We have hobbing, shaping, shaving, tooth chamfering and gear grinding capabilities. All drilling, milling, tapping and I.D. grinding is done in-house, enabling us to make gears more efficiently and economically and to maintain our scheduled delivery dates.

www.raycargear.com

THE PURDY CORPORATION

A leader in precision manufacturing for more than 50 years, The Purdy Corporation manufactures aerospace transmissions, large turbine engine components and other complex machined parts and assemblies of unsurpassed quality and value. We provide complete engineering and CAD/CAM; gear metrology; heat treat, metallurgical and non-destructive inspection; assembly and testing.

www.purdytransmissions.com

Klingelnberg GmbH

Visit the Klingelnberg site for links to specifications on the Klingelnberg products. Our contact in North America for all Klingelnberg products is: Liebherr Gear Technology in Saline, Michigan, at telephone (734) 429-7225.
Also visit *www.pointofprecision.com* and *www.sigma-pool.com*.

www.klingelnberg.com

SIGMA POOL

Visit the Sigma Pool site for links to specifications on the Sigma Pool range of CNC gear processing machines—hobbing, shaving, shaping, bevel gear generating machines and measuring centers. Our contact in North America for all Sigma Pool products is: Liebherr Gear Technology in Saline, Michigan, at telephone (734) 429-7225.

www.sigma-pool.com

CLASSIFIEDS

SERVICE

INTERSTATE TOOL CORP.
CLEVELAND, OHIO

CUSTOM ENGINEERED & MANUFACTURED CUTTING TOOLS ESTABLISHED 1960

FORM RELIEVED & PROFILE GROUND MILLING CUTTERS
GEAR SHAPER & SHAVING CUTTERS
ALL CLASSES OF HOBS
HSS. SOLID CARBIDE & CARBIDE TIPPED

WHETHER YOU NEED NEW TOOLS, MODIFICATIONS, RESHARPENING, REPAIRS OR M&M INSPECTIONS,
CONTACT US FOR A QUOTE TODAY!

www.interstatetoolcor.com
Tel: 216-671-1077 • Fax: 216-671-5431

CIRCLE 162

PRECISION GROUND GEARS

- Spur, Helical and Pump Gears to AGMA Class 15
- Featuring the latest grinding and CNC technology including:
  - Reishauer RZ300E Electronic Gear Grinders
  - Gleason TAG 400 CNC, 8-axis High Production Gear Grinder
  - Full CNC Multi-axis Cylindrical Grinding (Internal and External)
  - High Performance CNC Hobbing
- Continuous Process Improvement Utilizing SPC and Quality Planning
- JIT Delivery using Innovative Stocking Programs

800-447-2392
Fax: 716-874-9003
www.niagaragear.com
email:info@niagaragear.com

NIAGARA GEAR CORPORATION

CIRCLE 166

GEAR TOOTH GRINDING SERVICES

- Cost effective gear tooth grinding specialists
- Gear manufacturers are our only customers
- Prototype and production quantities
- Capacity to 27.5" P.D., 3.5 D. P.
- Able to match delivery to your requirements
- All service to AGMA standards with Certified Gear Inspection Equipment

PRO-GEAR COMPANY, INC.
23 Dick Road, Depew, NY 14043
Toll Free: 877-684-3810 • Fax: 716-684-7717
E-mail: *progearinc@aol.com*

CIRCLE 168

HOB SHARPENING SERVICE

Star Cutter Co.

Since 1927
Star®
STAR CUTTER COMPANY
ISO-9001 CERTIFIED

• THIN FILM COATINGS

West Branch Industries
Subsidiary of Star Cutter Co.
2083 W. M-55, West Branch, MI 48661
1-888-Resharp • 1-888-737-4277
Phone: (989) 345-2865 • FAX: (989) 345-5660

CIRCLE 169

HOB SHARPENING

INDEX TECHNOLOGIES

index TECHNOLOGIES

- AGMA Class AA
- Helical
- Skiving
- Carbide

-up to 1.25 N.D.P. capacity
-recoating & stripping of all coating types
-tool performance analysis
-rapid turnaround

Index Technologies Inc.
21135 Lorain Road, Fairview Park, Ohio 44126
Phone: 440-895-4627 (HOBS) Fax: 440-331-0516
Email: gallenco@msn.com

CIRCLE 160

GEAR TOOTH GRINDING SERVICES

Spur - Helical - Double Helical

Capacity up to 60.5" O.D., 1 D.P., 29" Stroke. All ground gears certified up to AGMA Class 14+ on Zeiss-Höfler 1602 CMM. Inventory of grinders includes Höfler 800, Höfler 1253 Supra, Höfler 1500, two Höfler Nova CNC 1000s (Fully CNC with on-board CMM checker), and Höfler Rapid 1000 Form Grinder.

Kreiter Geartech
2530 Garrow St., Houston, TX 77003
Phone: 713-237-9793 Fax: 713-237-1209
Contact: Mr. Willie Whittington
Visit our Website at
www.kreiter-geartech.com

CIRCLE 163

Rates—Line Classified: 1" minimum, $325. Additional lines $45 per line (8 lines per inch). Display Classified: 3" minimum: **1X**—$735, **3X**—$685 per insertion, **6X**—$645 per insertion. Additional per inch: **1X**—$255, **3X**—$235 per insertion, **6X**—$225 per insertion. **Color Classified:** Add $150 per insertion for color. *Gear Technology* will set type to advertiser's layout or design a classified ad at no extra charge. **Payment:** Full payment must accompany classified ads. Send check drawn in U.S. funds on a U.S. bank or Visa/MasterCard/American Express number and expiration date to *Gear Technology*, P.O. Box 1426, Elk Grove Village, IL 60009. **Agency Commission**: No agency commission on classified ads. **Materials Deadline:** Ads must be received by the 15th of the month, two months prior to publication. **Acceptance:** Publisher reserves the right to accept or reject advertisements at his discretion.

SERVICE

PRECISION GROUND GEARS

- **Bevel and Hypoid**
- **Spur and Helical**
- **Taper Rack and Pinion**
- **Worms & Wormwheels**

CURVIC® Couplings
(registered trademark of The Gleason Works)

SUDA International Gear Works Ltd.
P.O. Box 4, Pittsford, NY 14534 USA
Fax: (716) 385-8537
E-Mail: lgknndy@att.net
www.sudagear.com

ISO-9002 CERTIFIED

SIG
of Shizuoka, Japan
Est. 1944

CIRCLE 170

Induction Hardening

Specialists in Tooth by Tooth Contour Hardening of Internal
Spur, helical and bevel gears

Our gear hardening equipment includes 5 NATCO submerged process machines and 5 AJAX CNC-controlled gear scanning machines. Tooth by tooth gear hardening from .5DP-10DP, up to 15 tons, 200" diameter.

American Metal Treating Company
Cleveland, Ohio
Phone: (216) 431-4492 • Fax: (216) 431-1508
Web: ***www.americanmetaltreating.com***
E-mail: ***mark@americanmetaltreating.com***

Breakdown Service Available

CIRCLE 154

- **BROACH SHARPENING**
- **HOB SHARPENING**
- **SHAVING CUTTER GRINDING**
- **THIN FILM COATING**
- **CUSTOM HEAT TREAT SERVICE**

PICK UP AND DELIVERY IN MANY AREAS

Gleason Cutting Tools
CORPORATION

1351 Windsor Road, P.O. Box 2950
Loves Park, IL 61132-2950
Phone (815) 877-8900
Fax (815) 877-0264

CIRCLE 156

HOB SHARPENING

Frisby PMC, well known for manufacturing Precision, High-Quality Gears, now offers Precision-Ground Hob *Sharpening Service for High Speed* Steel or Carbide fine pitch hobs.

ISO 9002 CERTIFIED

Frisby P.M.C., Inc.
1500 Chase Avenue
Elk Grove Village, IL 60007-4880
Phone: 847/439-1150
Fax: 847/439-1164
Web Address: *http://www.frisby-pmc.com*

CIRCLE 155

GEAR TOOTH GRINDING

Spur • Helical
• Herringbone (with groove)
Capacity up to 63" O.D.,
1 D.P., 16" face

AGMA Certification Inspection
Delivery to Meet Your Requirements

Midwest Gear Corp.
2182 E. Aurora Rd.
Twinsburg, OH 44087
Phone 330-425-4419
Fax 330-425-8600

Direct your inquiries to
Ron Humphrey, General Manager
ronh@mwgear.com

CIRCLE 164

HELP WANTED

SALES/ENGINEER

PARKER INDUSTRIES (Long Island, New York) seeks sales-oriented Engineer with some knowledge of gear cutting tools and related products. Good technical and communication skills a must.

Reply in confidence with relevant information to:

George A. Parker
Parker Industries Incorporated
P.O. Box 465
Bohemia, New York 11716

PARKER

GEAR CALCULATION GEAR DEVELOPMENT

- Calculation
- Optimizing
- Expert Opinion
- Design
- Prototype manufacturing
- AGMA, ISO, DIN, VDI, GLEASON
- Metric and US measures

Software Distribution and Briefing

- HORNET -
The Way To Make Your Product Profitable

HORNET GmbH
Seewiesenstr.90, D-73329 Kuchen, Germany
Phone: (++49)-7331-981646 - Fax: (++49)-7331-981647
info@hornet-gmbh.com
www.hornet-gmbh.com

CIRCLE 157

HOB SHARPENING

- State-of-the-art CNC sharpening and inspection machines
- Wet grinding with free-cutting CBN or diamond wheels for "Burn free" sharpening of carbide or high speed steel
- Optional recoating and stripping
- Rush service available

Koepfer America, LLC

J K S

635 Schneider Drive
South Elgin, IL 60177
Phone 847-931-4121
Fax: 847-931-4192
sales@koepferamerica.com

CIRCLE 172

COMING SOON

FULL COLOR CLASSIFIED ADS!

CALL PAT FLAM AT
(847) 437-6604
TO RESERVE YOUR SPOT
TODAY!

...and visions of wormwheels danced in their heads

Does anyone know where we can find a gear-shaped fruitcake?

It's the holiday season again, and the Addendum staff has many friends. We'd like to get each of them the perfect holiday gift, something that demonstrates thought, caring and good will. Of course, we're looking for gifts with meaning, and for us, that can only mean gears.

To prepare for the gift-giving season, we've sent our team of personal assistants to shopping malls, corner boutiques and websites around the globe with a simple mission: Find the gears.

Because we know that many of you share our mindset, we've assembled a brief list of some of the gifts that will be sure to impress your loved ones this year.

GEAR TIES

Perfect for dads, husbands and male co-workers with gear fashion sense, The Lee Allison Co. of Chicago offers designer ties with a gear motif. These handmade ties are 100% woven silk and are available in burgundy/gold/ivory (shown), black/gray/silver and blue/green/gold, for $59. The company's owner, Lee Allison himself, has offered free shipping (within the United States) for *Gear Technology* readers. Just call 888-434-8437 and tell them you saw the tie in *Gear Technology*, or visit *www.leeallison.com* and type in the promotional code GEAR at checkout. If you visit the website, you can also view the other colors.

GEAR EARRINGS

For that special lady on your shopping list, Kar5 Jewelry, Gifts and Accessories, located in New York City, offers a unique variety of hand-crafted jewelry items. According to the company's website, this jewelry can "take you from a streetfight to the opera," which makes it perfect for a number of Addendum team relatives.

Pictured here are Kar5's gearstone earrings, available with either black stones or neutral stones, for $22 a pair. The earrings can be ordered from the company by calling (201) 656-2725 or by sending an e-mail message to *kar5jewelry@netscape.net*.

FOR THE KIDS

Gears!Gears!Gears! from Learning Resources Inc. of Vernon Hills, IL, is a line of gear-related learning toys for ages 3 and up. The 95-piece Gears!Gears!Gears! Building Set includes brightly colored gears, pillars, cranks, connectors and an interlocking base, available for $19.95 from *www.gearsgearsgears.com*, the company's website, or by calling 888-800-7893. Related accessories and building activity books are also available.

Learning Resources also offers motorized sets, including the Gearbotics™ Sonic T-Rex™, a 28-piece set for building a walking, roaring dinosaur. The set includes gears, connectors, dinosaur pieces and a motor with T-Rex sounds. It's available for $28.95 on the website. Other motorized sets include the Gearbotics™ Sonic Insect, Gearbotics™ Sonic Robot and Gearbotics™ Sonic Space Station.

FOR THOSE WHO HAVE EVERYTHING

We recommend that Internet-savvy shoppers visit Internet auction sites, such as eBay (*www.ebay.com*). We found a lot of gear-related items there, including some incredible bargains on gear games, gear toys, gear puzzles, gear jewelry, gear neckties and much more.

DOES ANYONE KNOW WHERE TO FIND GEAR WRAPPING PAPER?

Now that our shopping is almost done, we'd like to wish all of you a happy holiday season and a prosperous new year. We'd also like to remind you that it's better to give than to receive, and that the Addendum team's address is 1425 Lunt Ave., Elk Grove Village, IL 60007, U.S.A.—in case any of you come up with that gear-shaped fruitcake.

WARNING

Taking the advice of the Addendum team has been proven to cause loved ones to believe you have an unhealthy obsession with gears.

Tell Us What You Think . . .
If you found this article of interest and/or useful, please **circle 340.**
If you did not care for this article, **circle 341.**